

# **SUBICE - “Study of Under-ice Blooms in the Chukchi Ecosystem”**

## **Cruise report from HLY1401**

**Kevin R. Arrigo, Chief Scientist**  
*Stanford University*

### **Introduction**

Over the last several decades, Arctic Ocean ice cover has become substantially thinner and more prone to melting, extending the period of open water. Associated with the loss of sea ice on the Arctic shelves has been an increase in light penetration and a dramatic rise in the productivity of phytoplankton. Because sea ice and snow strongly reflect and attenuate incident solar radiation, the growth of phytoplankton at high latitudes is generally thought to be restricted to open waters of the marginal ice zone (MIZ) once sea ice retreats in spring. However, results from our recent ICESCAPE program contradict the paradigm that waters beneath the consolidated ice pack harbor little planktonic life. During two field campaigns in the Pacific sector of the Arctic Ocean, ICESCAPE discovered intense blooms of phytoplankton growing beneath fully consolidated sea ice. The phytoplankton biomass associated with these under-ice megablocks rivaled that of the most productive ocean ecosystems on Earth. A relatively thin sea ice cover with more numerous melt ponds enhanced light penetration through the ice into the upper water column, enabling phytoplankton blooms to develop when much of the Chukchi continental shelf was still covered in sea ice.

The primary objectives of SUBICE were to determine the spatial distribution of large under-ice phytoplankton blooms on the Chukchi Shelf and the physical mechanisms that control them. The project utilizes new data obtained from both remote instrumentation (e.g. moorings, satellites) and an interdisciplinary ship-based field program to gain a better understanding of the physical/chemical conditions that favor under-ice bloom development as well as the physiological adaptations that allow phytoplankton to flourish beneath sea ice.

The long-standing paradigm of the Arctic Ocean is one in which phytoplankton proliferate at the ice edge, supplying a substantial fraction of annual NPP and concentrating much of the food web in the MIZ. However, if under-ice phytoplankton blooms are widespread, then current estimates of annual NPP on Arctic continental shelves may be >10-fold too low. Our research program will allow us to determine the extent of under-ice blooms on the Chukchi Shelf and provide better estimates of production in these seasonally ice covered waters. It will also provide an improved understanding of the timing of phytoplankton blooms under the ice, in the MIZ, and in the open waters of the Chukchi Shelf, as well as the mechanisms controlling them.

### **Highlights of SUBICE**

There were three primary scientific objectives to SUBICE. Due to the early season timing and shortened duration of the cruise (relative to the 70 day cruise we proposed), these objectives were met with varying degrees of success.

#### *1) Characterize the nutrient distributions under the ice and the physics that control them.*

Previously, there was no information about the spatial extent and characteristics of the high-nutrient Pacific winter water over the ice-covered portions of the Chukchi Shelf at the end of the winter season. As such, we knew very little about the physical/chemical/biological processes that control nutrient distributions on the shelf during this critical time of the year when the ice begins

to thin and melt ponds develop. This information is essential for assessing where on the Chukchi Shelf conditions are suitable for the development of under-ice megablooms.

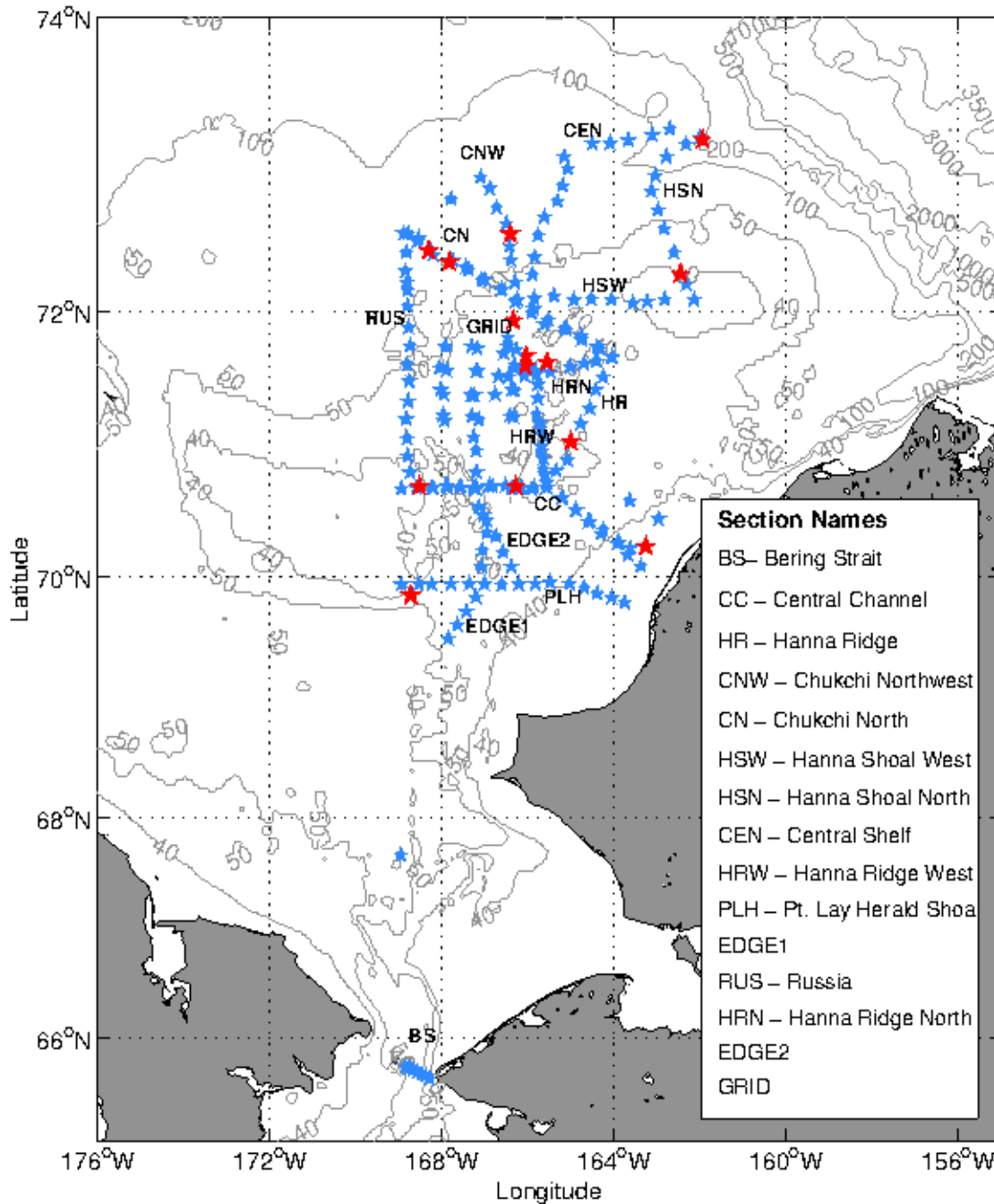


Figure 1. Map showing locations of hydrographic sections sampled during SUBICE. Ice stations (red stars) also included a full suite of hydrographic measurements.

High nutrient winter water enters through Bering Strait and then spreads into parts of the Chukchi Sea along advective pathways, while convection driven by brine-rejection occurs locally on the shelf. Both the local convection and the lateral advection of dense water are apt to stir up regenerated nutrients from the sediments into the water column. Prior to SUBICE, we had no idea about the relative importance of these local vs. remote nutrient sources and how subsequent mixing and advection dictate shelf-wide (lateral and vertical) nutrient distributions. These issues are being addressed using a combination of year-long mooring time series – both inside and outside of a known advective pathway – and extensive measurements of the hydrography, circulation, and nutrient content conducted during the recent SUBICE cruise.

Although the moorings have yet to be recovered, we successfully completed the first-ever comprehensive survey of the state of winter water in the Chukchi Sea shortly after the conclusion of the winter season (Figure 1). This enabled us to answer one of our primary research questions: Is the Chukchi Sea completely “reset” with high-nutrient winter water each year? We observed winter water with high nutrient concentrations throughout the water column all over the Chukchi Shelf, demonstrating that the system was indeed reset with nutrients throughout the region prior to spring. The entire system was poised for a phytoplankton bloom once melt ponds began to form and light levels increased to adequate levels.

Data collected during SUBICE should also allow us to address our other two research questions related to circulation and nutrient distributions: What are the relative roles of remote advection (from the Bering Sea) versus local convection in supplying the nutrients? and, How does the timing and evolution of the winter water dictate the availability of nutrients for NPP? High nutrient concentrations were observed both in the main circulation pathways and in the more quiescent areas in between, suggesting that there is a balance between nutrients advected from the Bering Sea and those regenerated on the shelf. More analysis will be done to determine the relative importance of these two processes.

*2) Determine the spatial variability and temporal evolution of the spectral light field above, within, and under the ice cover.*

During ICESCAPE, we found that the light field under a sea ice cover exhibits extreme spectral, spatial, and temporal variability. For example, under-ice light levels increase by two orders of magnitude during the seasonal transition from snow covered ice to ponded ice. Under melting ice, there can be a 10-fold difference in irradiance over just a few meters. During SUBICE, we were able to determine the light field above, within, and under the ice cover by measuring the optical and morphological properties of the ice cover. Optical measurements included spectral albedo, in-ice irradiance, and transmittance. Measurements covered the spectral range from the ultraviolet through the visible and will include the full range of ice conditions present.

The primary questions we wanted to answer related to sea ice optics included: How early in the season do ice optical properties promote phytoplankton growth under the sea ice? How does this timing vary with latitude? How important is light absorption by populations of ice-algae to the transmission of light through the ice to the water column below? Is there a critical melt pond fraction that is required for the initiation of an under-ice phytoplankton bloom?

Although we observed the onset of pond formation in only a few isolated cases, melt ponds did lower albedo from approximately 0.6 to 0.2 and increased transmission of visible light by a factor of 3.2. Unfortunately, a late season snowfall and northerly winds in the region combined to reset the albedo to a higher level and delay melt onset compared to recent years. As a result, there was little melt prior to the end of SUBICE and no under-ice phytoplankton bloom.

We were able to observe that light transmission through ice into the upper ocean was low, partially due to a late melt onset and remaining snow cover throughout most of the cruise, but

also due to large amounts of ice algae in place on the ice bottom, demonstrating that light transmission is markedly reduced by sea ice algal absorption.

3) *Characterize distributions and evolution of under-ice phytoplankton blooms in relation to the physical/chemical setting.*

Because the formation of melt ponds was delayed during 2014, light intensity was never high enough under the ice to stimulate the formation of an under-ice phytoplankton bloom. However, we were surprised to learn that even in waters covered with as little as 60-70% ice cover over a relatively wide area, phytoplankton blooms never formed in the water column. Hydrographic data suggest that even though light penetration into surface waters may have been sufficient for bloom formation, the cold temperatures facilitated high rates of convective mixing and the associated weak stratification allowed deep mixing even in the moderate wind fields we experienced. Thus, while we were too early to observe an under-ice phytoplankton bloom, we learned that high nutrients and high light transmission are not sufficient conditions for such a bloom to form – the waters have to stop mixing, allowing phytoplankton to bloom in the well-lit upper water column.

Research components of SUBICE. As originally proposed, SUBICE was composed of three primary research components that included 1) hydrography and circulation, 2) sea ice structure and optics, and 3) nutrient and phytoplankton distributions and phytoplankton physiology.

However, because of the ability of the USCGC *Healy* to support a large science team, we expanded the scope of the project (at no cost to NSF) to include a large number of other disciplines that we felt would complement our funded research. These other components included measurements of: atmospheric properties, concentrations of radium and trace metals in seawater, the carbonate system, bacterial abundance and production, microbial community composition and viral lysis rates, zooplankton abundance and grazing rates (on phytoplankton and bacteria), water column optics (including absorption by CDOM and particles), and sterol and IP<sub>25</sub> biomarkers in the ice, water column, and sediments.

Summaries of all the subcomponents of SUBICE are provided below.

## Hydrographic Measurements and Shipboard Velocity Data

**Robert Pickart, Frank Bahr, Carolina Nobre, Elizabeth Bonk, Maria Pisareva, William Pickart**

*Woods Hole Oceanographic Institution*

**Astrid Pacini**

*Yale University*

### **Objectives**

The Woods Hole Oceanographic Institution component of SUBICE addressed the physical state of the Chukchi Sea during the 42-day mission aboard USCGC *Healy* (cruise HLY1401). The measurement program consisted of conductivity-temperature-depth (CTD) casts, dissolved oxygen analysis, and shipboard velocity measurements. The *Healy's* 12-position 30-liter Rosette system was used, with dual temperature (SBE3) / conductivity (SBE4c) sensors, a 0-10,000 psi Digiquartz Pressure sensor, a SBE43 oxygen sensor, a WET Labs ECO-AFL/FL fluorometer, a WET Labs C-Star transmissometer, a Biospherical/Licor QSP-2300 PAR sensor, and a Benthos PSA-916 altimeter. Direct velocity measurements were made using *Healy's* hull-mounted Acoustic Doppler Current Profiler (ADCP) systems: the Ocean Surveyor 150 KHz unit (OS150) and the Ocean Surveyor 75KHz unit (OS75). Since most of the SUBICE program took place on the shallow Chukchi shelf, we relied principally on the OS150.

This section details the processing and analysis of the hydrographic data and vessel-mounted ADCP data carried out by the WHOI team. During SUBICE, 230 CTD stations were occupied in the Chukchi Sea comprising 16 high-resolution transects, two occupations of a square grid, and a number of miscellaneous stations (Figure 1). In addition, CTD casts were done at all of the ice stations. Preliminary vertical sections of hydrographic variables were produced during and/or shortly after the conclusion of each transect. Following this, more complete vertical sections were constructed that included water sample data, absolute geostrophic velocity, and bottom depth information from *Healy's* depth sounders. After the cruise the CTD temperature and conductivity/salinity data will be calibrated and quality controlled (no further editing will be done on the other CTD variables). The water sample measurements will be merged with the CTD bottle stop data into a WOCE format data file. These data products will be made available shortly to the science party via the SUBICE website. The vessel-mounted ADCP will be posted to the website at a later date.

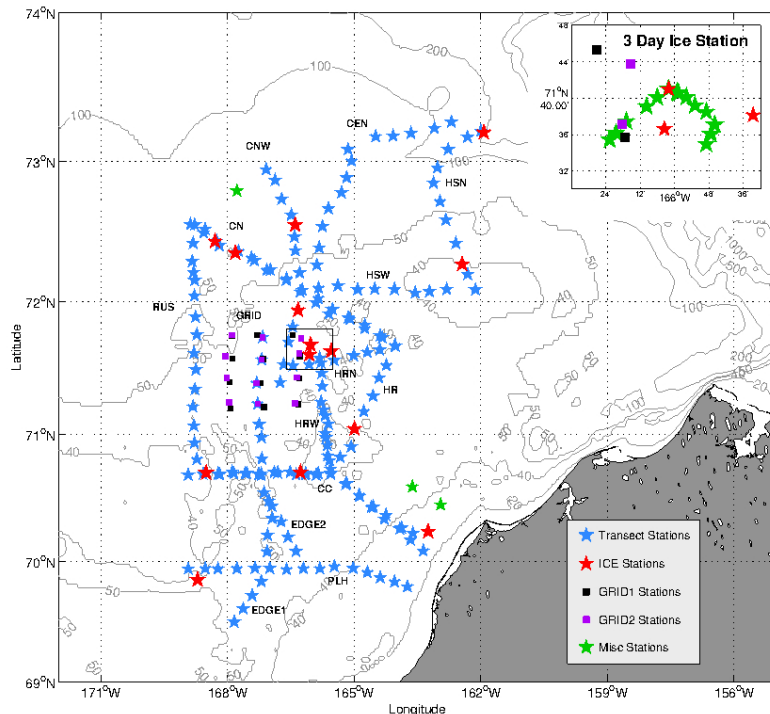
### **Hydrographic Component**

#### **1) CTD Data**

A total of 251 CTD casts (over the 230 stations) were carried out using the sensor setup described above. Upon completion of each cast, an automated set of scripts was run to produce a 1db pressured-averaged downcast file of the different variables. The beginning downcast scan number recorded by the CTD console operator was used in the Datcnv processing program to strip out unwanted data during the initial soaking period of each cast (while the conductivity pump was turning on). The batch file processing program also generated a running log of the CTD casts (station number, name, date, time, latitude, longitude, uncorrected water depth). The pertinent products from the batch file processing were immediately transferred to the public server on the *Healy*. As mentioned above, the final CTD data set will be posted to the SUBICE website shortly.

#### **2) Oxygen Measurements**

Oxygen samples were collected from the Niskin bottles at 208 stations, using the following procedure. Brown ground glass stoppered bottles were rinsed and filled to overflowing twice the volume of the bottle, taking care to minimize bubbles. One milliliter of 3N MnCl<sub>2</sub> followed by



one milliliter of 8N NaI-NaOH was added to the sample. The bottles were then stoppered and vigorously shaken 15 times. The flocculate was allowed to settle to the bottom of the bottle and then the bottle was shaken again 15 times. When the flocculate had settled for a second time the samples were acidified with 1 milliliter of 10N H<sub>2</sub>SO<sub>4</sub>, and shaken for a final time. After all of the precipitate was dissolved, a known volume was dispensed from a pipette into a 100 mL glass beaker. This was then titrated using an automated Winkler system. The oxygen data are included in the cruise water sample file as described below.

Figure 1: Zoomed-in view of the CTD and ice stations occupied north of Bering Strait during SUBICE. The region of the 3-day ice station is enlarged in the upper right-hand corner of the plot. Transect names are indicated in the key of Figure 1a.

## 2) Water Sample Data

In order to facilitate the analysis of water properties done by the different research groups in SUBICE, a merged water sample file was generated. The file contains a selection of CTD measured properties from the up-cast trace, as well as all water sample variables that were available during the cruise. It is anticipated that additional variables will be added to this file post-cruise.

Two file types were generated. One follows the WOCE WHP (csv) format guidelines and the other is as a tab-delimited text file with two header lines followed by columns of ascii data. The former is intended for submission to NODC or other data centers, and the latter was designed for easy loading and manipulating in MATLAB and other data processing software.

The water sample variables included in the merged files are salinity, oxygen, chlorophyll, nitrate, phosphate, silicate, nitrite, and ammonium. The two files will be available shortly after the cruise on the SUBICE website.

## II. Velocity Component

### 1) ADCP system

#### 1.1) Instrumentation and supporting hardware

*Healy* has two shipboard Acoustic Doppler Current Profilers (ADCPs): A 75KHz phased array Ocean Surveyor (OS75) for extended vertical range, and a 150KHz instrument that is better

suited for shallow water. In recent years, efforts by the ship's personnel and by the STARC science support (e.g., re-routing of the transducer cables to reduce electrical noise) significantly improved their performance by increasing the signal to noise ratio. For this cruise, we never exceeded the profiling range of the OS150, and therefore focused on this instrument with its finer vertical resolution.

Since the ADCP attempts to measure relatively small current signals from a much faster moving instrument platform (the ship), good position and in particular heading information is vital to obtain accurate velocity estimates. *Healy* has several GPS position devices. However, the previous primary ADCP heading device, a POSMV system, experienced extensive drop-outs early in the cruise. We therefore switched to the ship's MK39 gyro compass. Fortunately, comparisons to the POSMV when it was operational demonstrated that the MK39 was not subject to the typical gyro errors triggered by ship's accelerations (Schuler oscillations), presumably because the MK39 includes a Motion Reference Unit (MRU; Scott Hiller, pers. comms.).

## 1.2) Software

Data acquisition software for collecting and combining the various data feeds is the final component of the ADCP system. *Healy* uses the UHDAS package, developed and supported by E. Firing and J. Hummon (University of Hawaii). This software is presently used by the majority of the UNOLS fleet. J. Hummon routinely visits the ship during the spring shake-down period for software and computer support. She also repeatedly provided email assistance during our cruise.

The OS150 collected 5-minute ensemble averages using standard acquisition parameters that included 4m vertical bins and 7m blanking below the transducer. Together with the 8m transducer depth, this placed the center depth of the first vertical bin at 19m. Based on past experience and recommendations by Hummon, we only collected in narrow band mode.

## 2) Onboard data processing and display

The data processing tasks consist of two basic steps: (i) converting ship-referenced measurements into estimates of earth-referenced currents; (ii) editing of outlier bins.

For the first task we used standard tools of the CODAS processing software, which is freely available and can be downloaded from <http://currents.soest.hawaii.edu>.

We began the first step with a check on the ADCP calibration, for which we collected bottom track (BT) data shortly after our departure from Dutch Harbor. This confirmed the existing OS150 transducer alignment setting of 28.4 degrees. BT was then turned off to instead collect additional water track pings. The only calibration adjustment consisted of a minor change to the default heading correction from 0.0 to 0.5 degrees after this improvement became apparent during the extended POSMV drop-outs. Next, routine CODAS tools rotated the ADCP data from the ship reference frame into geographic coordinates, and removed the ship velocity to derive absolute current estimates. Finally, we employed the COAS model to remove barotropic tides (Gary Egbert and Lana Erfeeva, OSU, <http://volkov.oce.orst.edu>).

The presence of ice caused major editing issues during the next task. With the help of the new CODAS tool "gautoedit.py" as well as additional MATLAB routines, we utilized typical quality parameters such as backscatter strength, percent good, and error velocity as well as consistency among neighboring profiles to remove ice interference. Typically, only on-station profiles provided acceptable data when the ship was in the ice. However, some of the early on-station profiles included anomalous velocity jumps, perhaps capturing water pulses from the ship's props during early station keeping adjustments. We speculate that the shallow water depths of the Chukchi Sea contributed to the strength of these apparent contaminations. Shallow

water also kept CTD profiling time short, reducing on-station time and thus the number of good profiles to compare. We adopted a strategy under which we would spend a minimum of 30 minutes on station to allow for good ADCP sampling.

### 3) Data display and access

The above steps generated time series of velocity profiles. These will be used to generate both lateral vector maps (for example, see Figure 2 below) and vertical sections of along-track and cross-track velocity.

These products, as well as the data, will be available after the cruise via the SUBICE website.

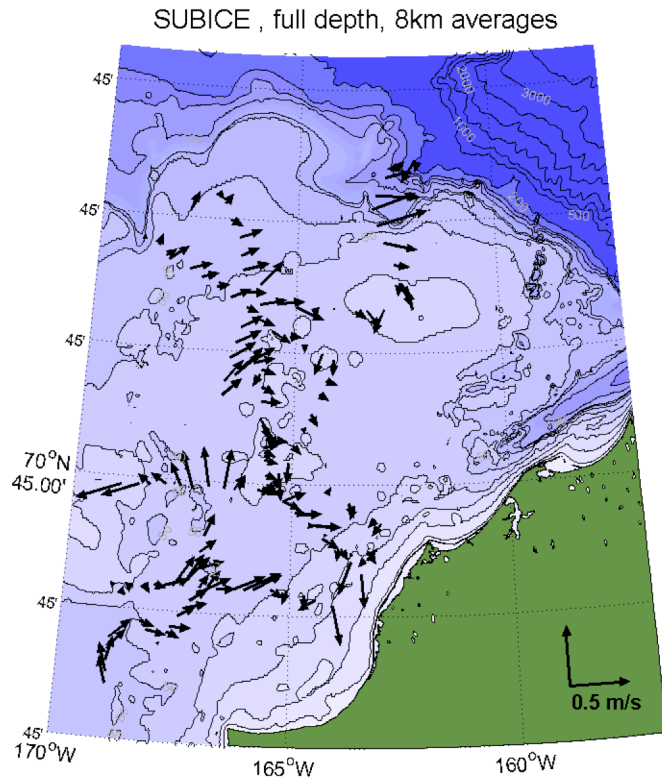


Figure 2. Vector maps created from ADCP data collected during SUBICE.

## **Sea Ice Physical and Optical Properties**

**Chris Polashenski and Don Perovich**

*Cold Regions Research and Engineering Laboratory / Dartmouth College*

**Carolyn Stwertka, Alexandra Arnsten**

*Dartmouth College*

**Ken Golden**

*University of Utah*

### **Objectives**

The overall goal of the ice physics work package was to obtain a dataset describing the state and spatial variability of the morphological and optical properties of the first year ice in the Chukchi Sea as the ice passed through the onset of spring melt. Particularly, we set out to capturing the transition in ice properties relevant to light transmission into the upper ocean, and to track the availability of transmitted light beneath the ice in the upper ocean during the time period encompassing the onset of snowmelt and formation of melt ponds on the ice surface.

### **Methods**

There were two broad classes of ice activities: on-ice measurements at individual floes and continuous observations made while the ship was in transit.

A total of 17 sets of on-ice observations were made at 12 ice floes, including one floe where we conducted 4 consecutive day's measurements and two later 1 day sets of observations. The on ice observations consisted of surveys and point measurements of sea ice morphology and optics. (see Table 1 for a summary of activities conducted during each set).

The optical observations were designed to provide a detailed characterization of the upwelling and downwelling components of the spectral radiation field from just above the surface through the ice and into the upper few meters of the ocean. Spectral albedos and transmittances, as well as transmitted vector and scalar PAR were measured. Optical observations were made at sites selected to encompass the full range of ice types and surface conditions encountered on the cruise. Special attention was paid to investigating the spatial variability of light transmitted through ice with varying snow cover depth, ice thickness, and, when available, bare and ponded ice. The overall pattern of albedo surveys included a 100-200m long transect line along which observations were taken every 2.5m, observations coincident with transmission measurements, and ad hoc investigations of surface types of interest. Transmission observations were logistically more limited in scope, and typically included measurements at 12-60 sites accessed through 2-5 boreholes. AOP and IOP measurements in the upper ocean were conducted coincidentally with these transmission observations by Guslain Becu of the Takuvik Group. Spectral albedo observations were collected with an ASD Fieldspec Pro 4. Transmission observations were collected with TRIOS Ramses spectroradiometers and LICOR vector and scalar PAR sensors deployed on a mechanical arm apparatus that positioned them just beneath the ice, 2 meters away from the borehole. Rotating the arm allowed access unique areas of ice from each hole. In addition to undisturbed observations, albedo and transmission at most sites were observed before and after removal of the snowpack to allow separate calculation of snow and ice extinction coefficients. Coincident measurements of ice algae chlorophyll concentrations (Arrigo group) and light transmission were collected to better understand the role that ice algae

play in restricting light availability in the upper ocean and the response of ice algal biomass to light availability.

The morphology component of the on-ice work included measurements of snow depth, ice thickness, ice temperature, salinity, porosity, and ice permeability. Surveys of ice thickness and snow depth were conducted using an electromagnetic induction sensor (EM31) and a Snow-Hydro Magnaprobe, respectively. The surveys were coincident with albedo and transmission observations, along transects 100-200 m long, with the survey pattern depending on the size and morphology of the individual floe. Where time allowed, additional thickness and snow depth observations were taken across larger areas of the floe to estimate floe scale variability in these properties. Transects of manual thickness measurements at 10-30 boreholes were conducted coincident with EM31 observations at many sites in order to check instrument calibration as ice salinity changed. When conditions allowed, an InfiniteJib remote controlled hexacopter was used to capture aerial photos of the site environment, further extending our ability to extrapolate the surface conditions at our optical sites to a floe scale. Cores were taken at each site for temperature, salinity, crystallography, and porosity. Upon removal, holes were drilled into the center of one core at 10 cm intervals for temperature measurements with a hand held thermistor probe. A second core was removed and immediately sectioned into 10 cm increments and bagged for melting and salinity measurements. An additional ice core was collected from each site to be shipped home to the laboratory for further optical measurements and analysis, including crystallography, dust, and sediment concentrations. Finally, handheld CTD casts were made at a number of sites using the array of boreholes created for other observations to assess ocean warming and freshening in the layer of water immediately beneath the ice, not typically accessible from ship borne observations.

Permeability studies focused on understanding movement of meltwater through the ice, and how pond formation during the early season is impacted by ice permeability. At each site 3-5 partial boreholes were drilled, lined with a casement pipe and subjected to positive and negative hydraulic head slug tests to assess the permeability of the underlying ice. Salinity of input water in positive head slug tests was varied to simulate variability in the mix of snow and ice melt entering the ice. Change in level within the casement lined boreholes was observed with a pressure-based level logger installed at the bottom of the tube.

While in transit, an ice watch characterizing the ice conditions at two-hour intervals was conducted while the ship was in the ice. The ice watch was made in cooperation with the Takuvik team (particularly Guislain Becu, Pierre Coupel, Joannie Ferland, Guillaume Meisterhans, Sophie Renaut, Jodi Sperling (outreach team)). The ASSIST standard Arctic observational protocol was used and the ice type, ice thickness, ice concentration, and pond fraction were recorded for the primary, secondary, and tertiary ice types encountered. Additional information including the state of melt, sediment content, algae concentration, and fauna present was also collected. Photographs of ice conditions were taken in conjunction with each ice watch, augmenting the ongoing collection of minutely photos from the ship's aloftcon system. These data provide a broad spatial overview of the properties of the ice cover in the Chukchi Sea during the cruise.

In-transit measurements were also made of absolute incident spectral solar irradiance and spectral reflectance of open ocean. The incident spectral irradiances were measured under sky conditions ranging from clear skies to complete overcast with fog. These observations will assist in determining the solar input to the ice – ocean system during the cruise.

## Preliminary Findings

### *Ice Optics*

#### *Albedo*

Figure 1 presents spatially averaged spectral albedo observations at each observation site over the duration of the cruise. Earlier curves are colored in darker blues while later season curves pass toward red. Characteristic changes in the spectral albedos can be seen with the onset of snowmelt (Infrared albedo drops to near 0), exposure of bare ice (visible albedo gradually declines toward 0.7) and pond formation (visible albedo drops by ~0.4 at pond sites).

An overall trend of gradually decreasing albedo is apparent over the course of the expedition. This trend is

interrupted in particular by a snowfall and cooling on June 5-6, and spatial variability due to ship transits to new ice floes. The highest albedo recorded was on 24 May, 2014 and the lowest was on 9 June, 2014 with the wavelength-integrated fraction of light reflected dropping from 85% to 53%. The transect on 24 May was dominated by deep snow and ice over 1m thick. The transect on 9 June included a large section of thin ice with meltpond formation underway. This was manifest as a layer of brackish water approximately 30cm deep beneath a thin (~4cm) surface ice crust. The southerly location of this ice, where it was subject to warm ocean water and warmer atmospheric conditions at the ice margin, likely contributed to its more advanced state of decay.

The temporal evolution at the floe we revisited 3 times during the cruise (June 3-6, 15, 17) shows the slow onset of melt without the added signal of spatial variability (Figure 2). Steady decrease in albedo June 3-5 is followed by a reset to high values after a late season snowfall June 6. Melt ponds were not seen until 15 June, but the appearance of a few scattered melt ponds and rotten ice caused a decrease in the spatially averaged integrated albedo from 0.78 (6 June) to 0.61 (15 June) on this floe, indicating that earnest melt pond formation likely began just as we departed.

With the slow onset to melt, an interesting sub-surface ‘pond’ formation was widespread. As air temperatures remained below the freezing point, loss of sensible and longwave radiation kept the surface frozen, but absorption of shortwave radiation within the upper ice combined with a lower freezing point due to slightly higher salinity contributed to the formation of a sub-surface liquid water layer. By the time of our departure from the last ice station, large areas of the thin

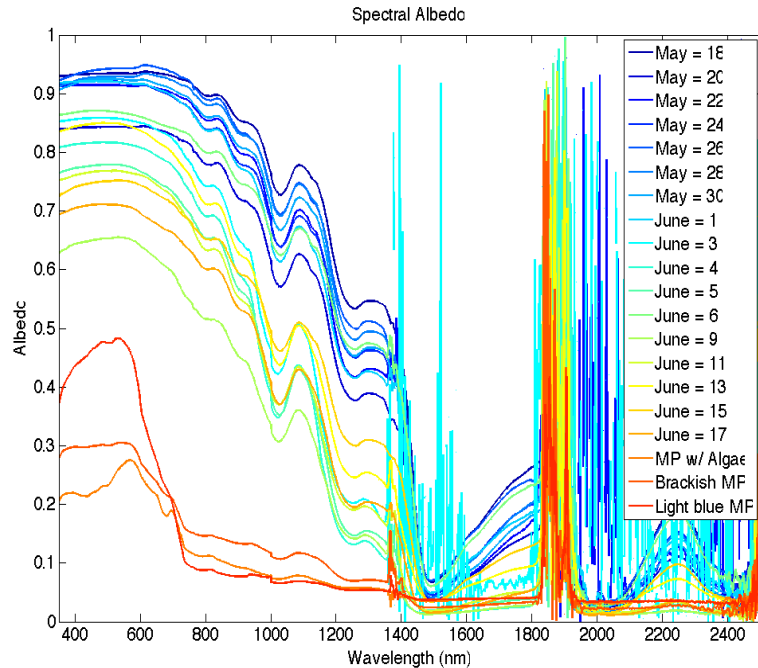


Figure 1. Total spectral albedo average of all floes sampled during SUBICE 2014. During the early part of May, the albedo signature represents snow that is optically thick and reflects over 90% of incoming solar radiation in the visible bands.

ice crust surface would break through this layer when stepped on and the impact of the layer on lowering albedo was apparent. A short period of warmer temperatures will likely remove the tops from these ‘proto ponds’.

The trend toward lower albedo is perhaps more readily visualized using the wavelength integrated albedo (Figure 3 blue line). The steady decrease in integrated albedo is interrupted by snowfall on June 5-6. A renewed drop on June 9+11 is largely due to transit south toward the ice edge. Returning north on June 13 - 17 resumes the steady decline from the melt reset observed at the three day ice station. The impact of snow depth (plotted in purple) on albedo is readily apparent in the strong correlation.

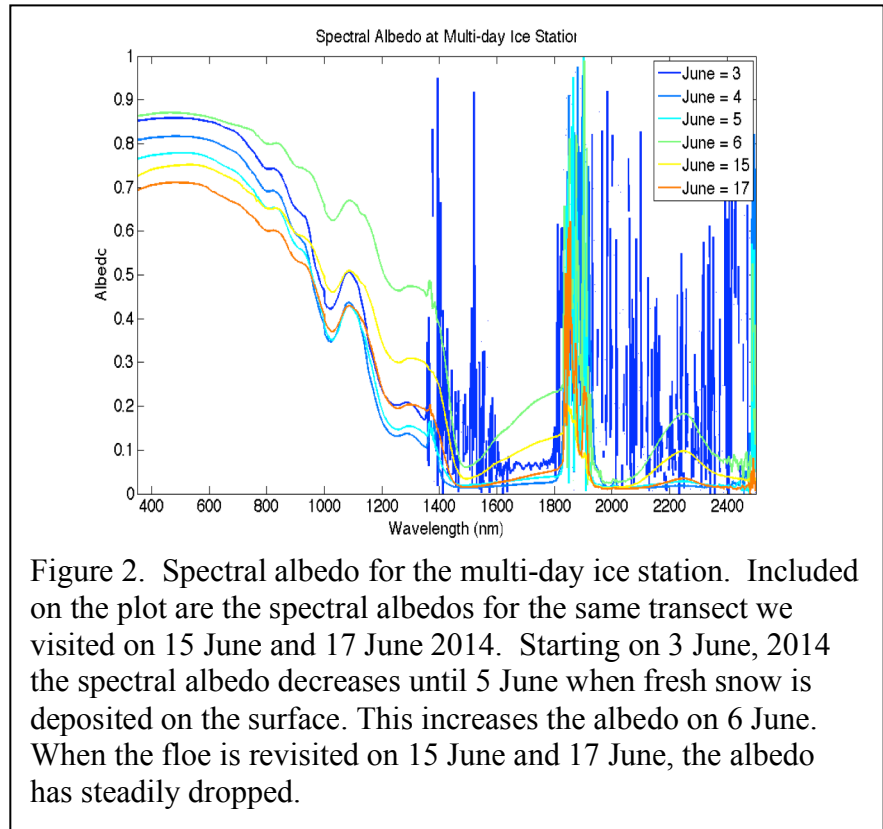


Figure 2. Spectral albedo for the multi-day ice station. Included on the plot are the spectral albedos for the same transect we visited on 15 June and 17 June 2014. Starting on 3 June, 2014 the spectral albedo decreases until 5 June when fresh snow is deposited on the surface. This increases the albedo on 6 June. When the floe is revisited on 15 June and 17 June, the albedo has steadily dropped.

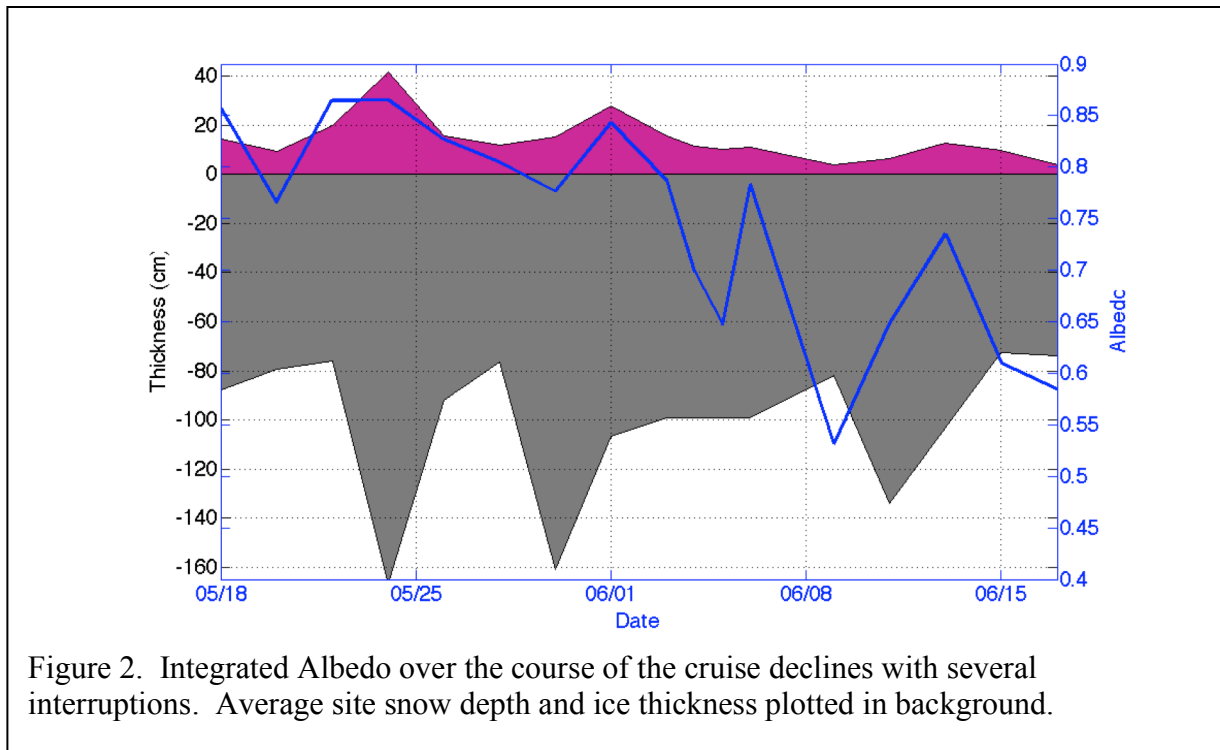


Figure 2. Integrated Albedo over the course of the cruise declines with several interruptions. Average site snow depth and ice thickness plotted in background.

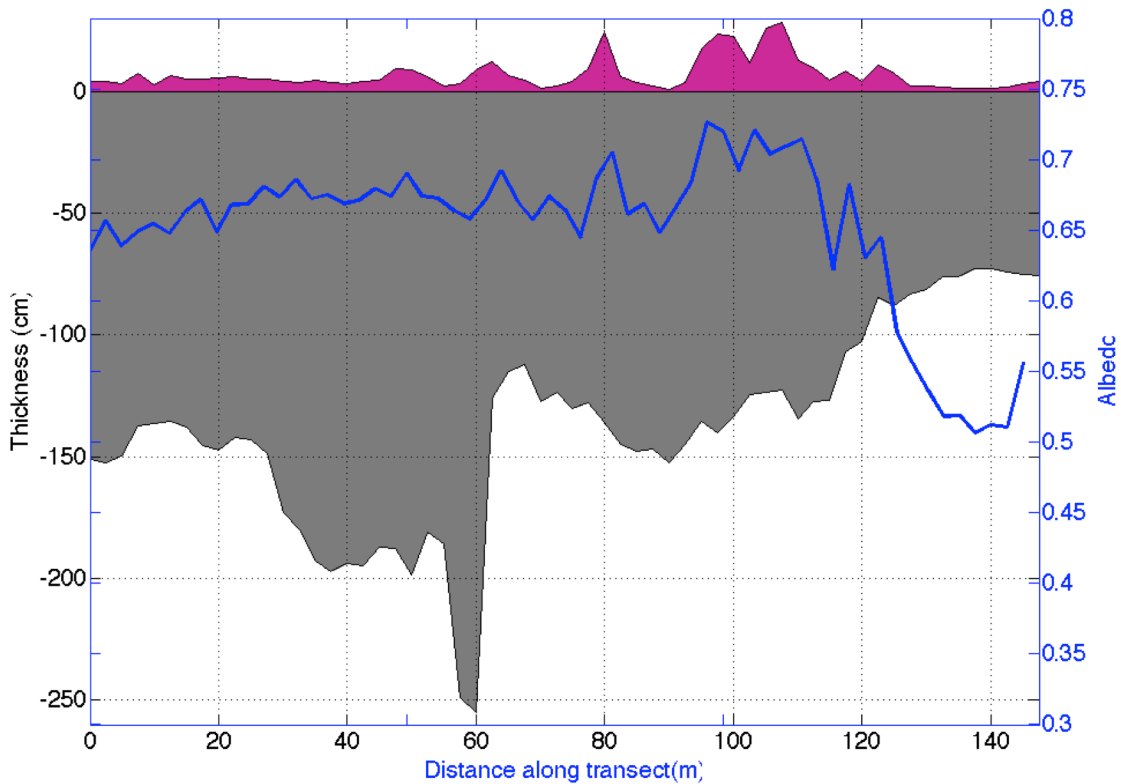


Figure 4. Example of a spatial variability transect along a 150m line on 11 June 2014. The grey color is the sea ice thickness measured with the EM31 and the magenta is the snow depth measured with the Magnaprobe. The transect starts out on a thick FY deformed floe. The transect goes over a series of deformed features at 40 m, 65 m, 80 m, and then a large ridge from 90-110 m which separates the deformed thick floe from a thinner FY undeformed floe which was more representative of the area. The albedo starts below 0.65 and increases to almost 0.7 as the snow gets thicker (to 15 cm). Once on the undeformed floe, the snow depth is close to zero and the albedo drops to 0.5.

Finally, Figure 4 shows the coincident collection of ice morphology properties such as thickness and snow depth alongside albedo. Adding coincident transmission and algae biomass observations collected at some sites will provide substantial opportunity for model based synthesis going forward.

### Transmission

Light transmission through the ice into the upper ocean also increased in line with dropping albedos, but remained well below those seen during the 2010-2011 ICESCAPE missions. Even the lack of pond formation and late presence of snow cover did not fully account for the low transmission. Bare ice transmittances were appreciably lower than expected.

Strong signatures of chlorophyll absorption were apparent in the transmitted spectra at most sites (Figure 8), indicating light absorption by ice algae was very important in controlling the transmitted light availability beneath the ice. Visual inspection of the ice bottom showed that all sites except site 84 were richly covered in ice bottom algae (see

Figure 7 photos). The unique case of site 84 therefore provides an interesting comparison. This station was the only multiyear ice sampled on the cruise and was site of the highest observed ice thickness and highest observed average snow depth at a transmission site. By ice properties alone, it should have the lowest observed transmittance, however measured PAR transmission at this site was 1.8 % of incident light while the preceding site indicates a measured PAR of just

0.25% with only 52% of the ice thickness and 43% of the average snow depth. Figure 5 shows the large difference in transmission curve between the algae-free case and three sites taken in close spatial and temporal proximity. Note the large drop in transmittance throughout the visible spectrum.

Transmitted PAR values are also plotted in Figure 6, showing the steady increase in through-ice transmission. This corresponded to a lowered albedo as surface melt progressed in removing snow cover and forming ponds,

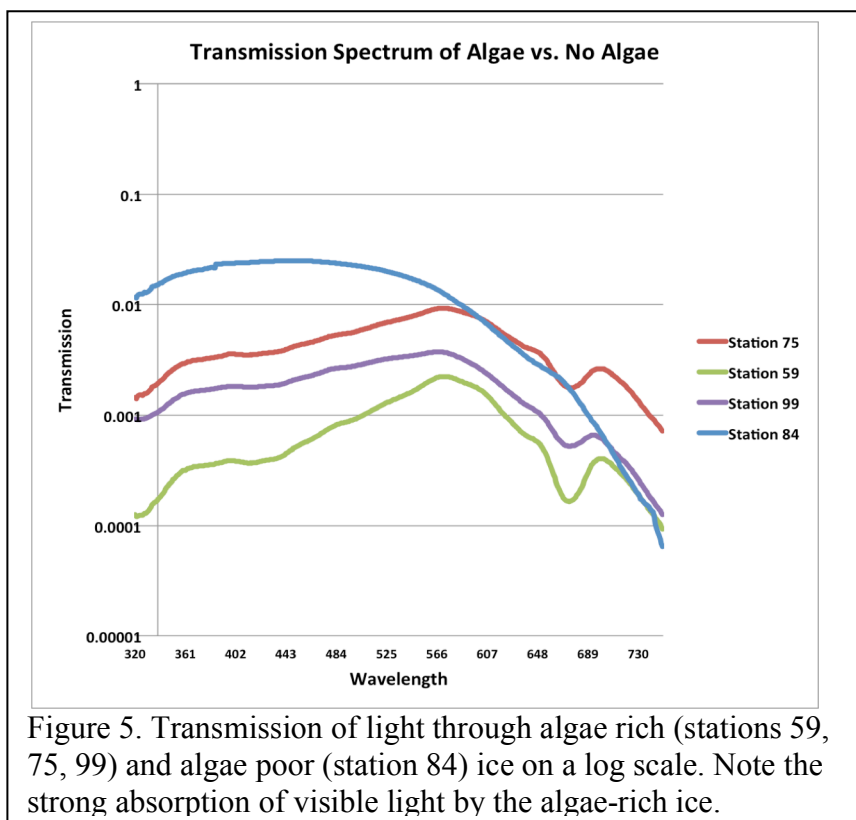


Figure 5. Transmission of light through algae rich (stations 59, 75, 99) and algae poor (station 84) ice on a log scale. Note the strong absorption of visible light by the algae-rich ice.

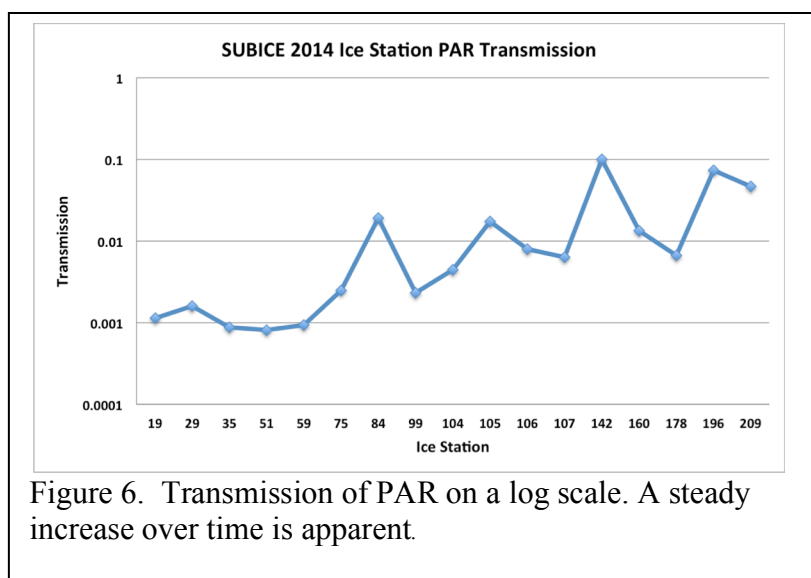
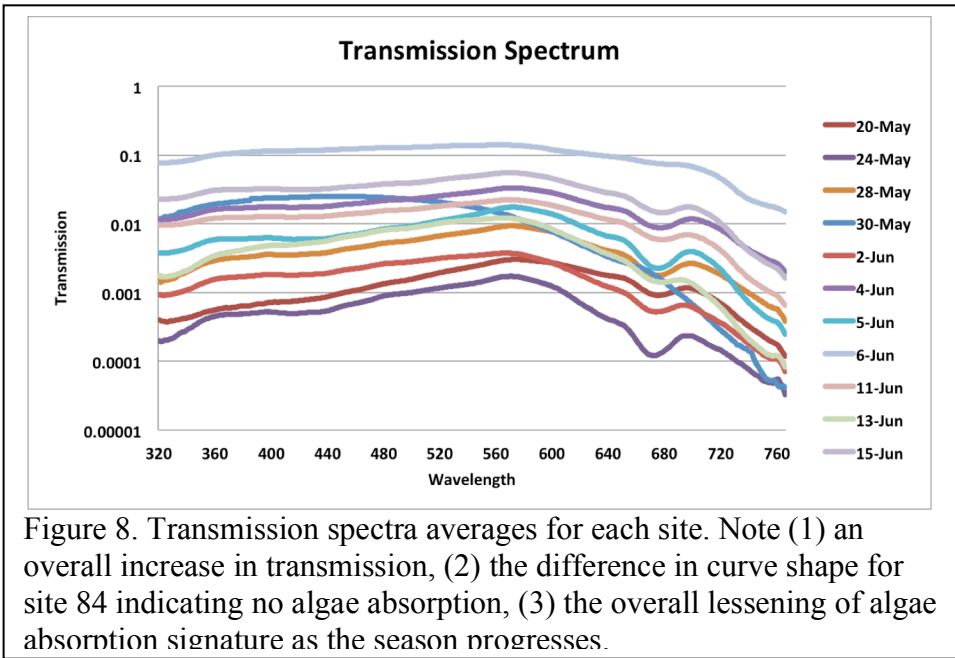
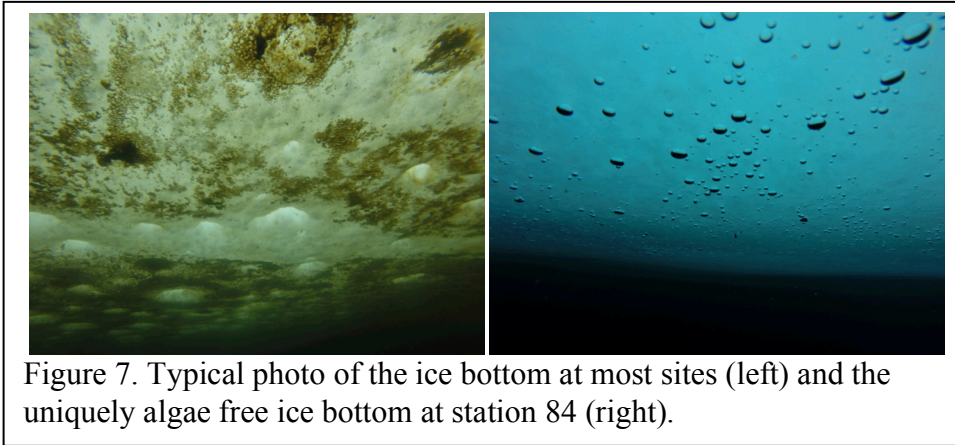


Figure 6. Transmission of PAR on a log scale. A steady increase over time is apparent.

but also to the gradual sloughing off of ice bottom algae. Further analysis is needed to partition the effects of ice algae and ice surface conditions on underice light availability.



*Ice Permeability*

Figure 10 shows the results of permeability tests conducted throughout the cruise using pore water (a natural, unmanipulated permeability test). Considerable scatter is caused by the heterogeneity of the internal ice structure. Warm ice encountered frequently had large (cm scale) pore spaces. The important component of this result is that permeability observed is universally too great for the formation of above ice melt ponds (which requires percolation constant  $k_z$  below  $10^{-12}$ ). That melt ponds typically form well above freeboard on ice of similar properties highlights a gap in our understanding of ice permeability and melt pond formation

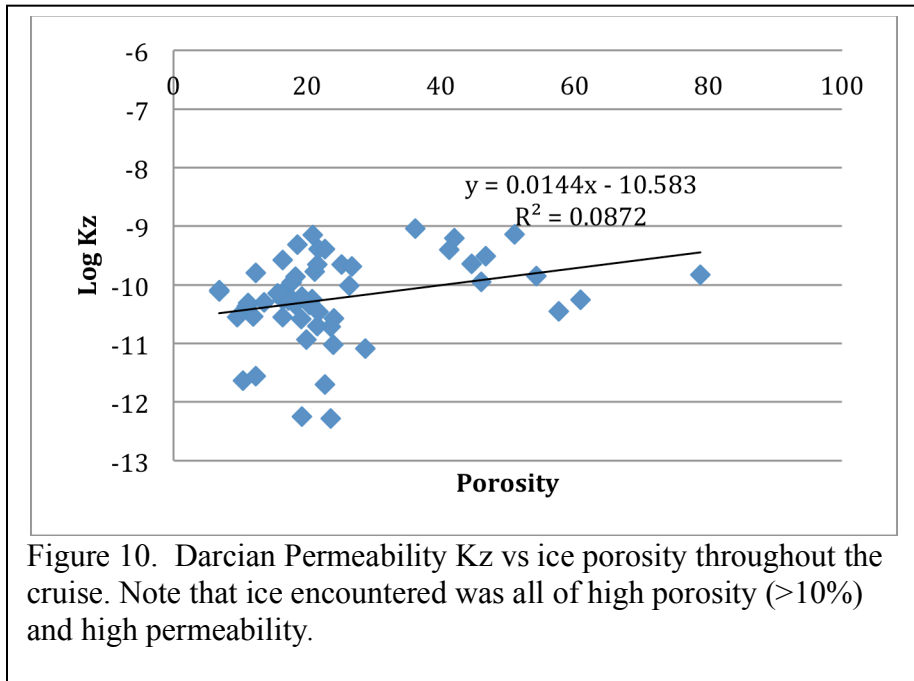


Figure 10. Darcian Permeability  $K_z$  vs ice porosity throughout the cruise. Note that ice encountered was all of high porosity (>10%) and high permeability.

Further experiments manipulating the salinity of water flowing into boreholes showed how ponds are able to form on such otherwise permeable ice by resealing pore spaces. Results of a typical borehole drainage experiment are shown in Figure 11 and 12. The test, conducted May 26<sup>th</sup>, consist of two adjacent test casements in a sheet of homogeneous, level, thermodynamically

formed first year ice 119cm thick. Water level in the casement tube is raised by the addition of water, then monitored as it returns to the freeboard level. Water head drops according to exponential decay as water percolates into the ice through the open bottom of the tube. Over time, multiple additions of water are conducted and each allowed to drain back to freeboard. The

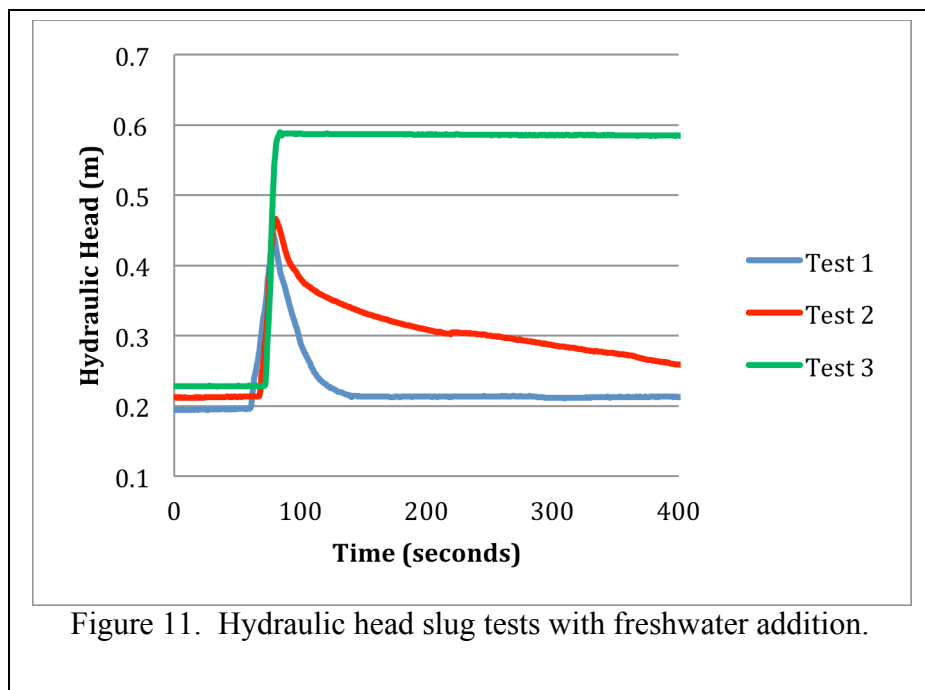


Figure 11. Hydraulic head slug tests with freshwater addition.

minimum temperature in the ice column at the time of this site was  $-2.1^{\circ}\text{C}$ , corresponding to a brine concentration in the pore space of 41 psu. Infiltrating water fresher than this concentration should result in ice growth within pore space upon intrusion, while water saltier should erode and enlarge the pore space, enhancing flow-through. Accordingly we added water with a higher salinity of (57 psu) to one borehole (Figure 12) and water with lower salinity (0.3 psu) to the other (Figure 11). In both cases the water was added at its salinity-determined freezing point,  $-2.9^{\circ}\text{C}$  and  $0.0^{\circ}\text{C}$  respectively.

The result is stunningly clear. The ice at this point in the year is highly permeable and added water drains out. The high salinity water percolates through the ice rapidly, with the hydraulic head decaying to approach original freeboard in a matter of a few minutes. Repeated additions of saline water behave similarly, but each subsequent addition percolates out

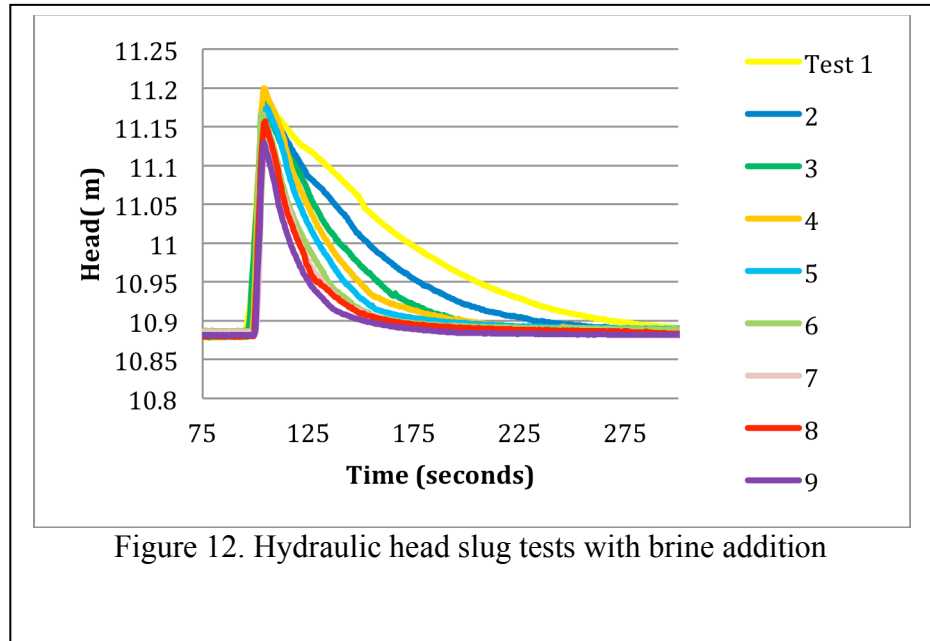


Figure 12. Hydraulic head slug tests with brine addition

faster the one before it, indicating that the cold, saline water is actually eroding the microstructure of the ice and enhancing the flow pathways. In contrast, fresh water blocks percolation. Once the  $\sim 1000\text{ml}$  of standing water in the casing has been displaced, the drainage rate slows, and very soon drainage ceases altogether, the percolation pathways having been plugged by refreezing fresh water.

Further analysis of the data we collected with varying salinity of infiltrating waters on various ice types should allow us to comment on the importance of freshwater snowmelt availability in sealing the ice surface, and forming melt ponds – a critical physical control over light availability.

### Ice Watch Observations

Results from the ice watch observations are plotted in Figure 13. The regional trends in ice properties are readily apparent from the observations, particularly including enhanced deformation and sediment entrainment in the coastal ice zone, greater thickness and snow depth near and among the multiyear pack at the northern end of our operation area, and widespread ice algae colonization throughout the study area.

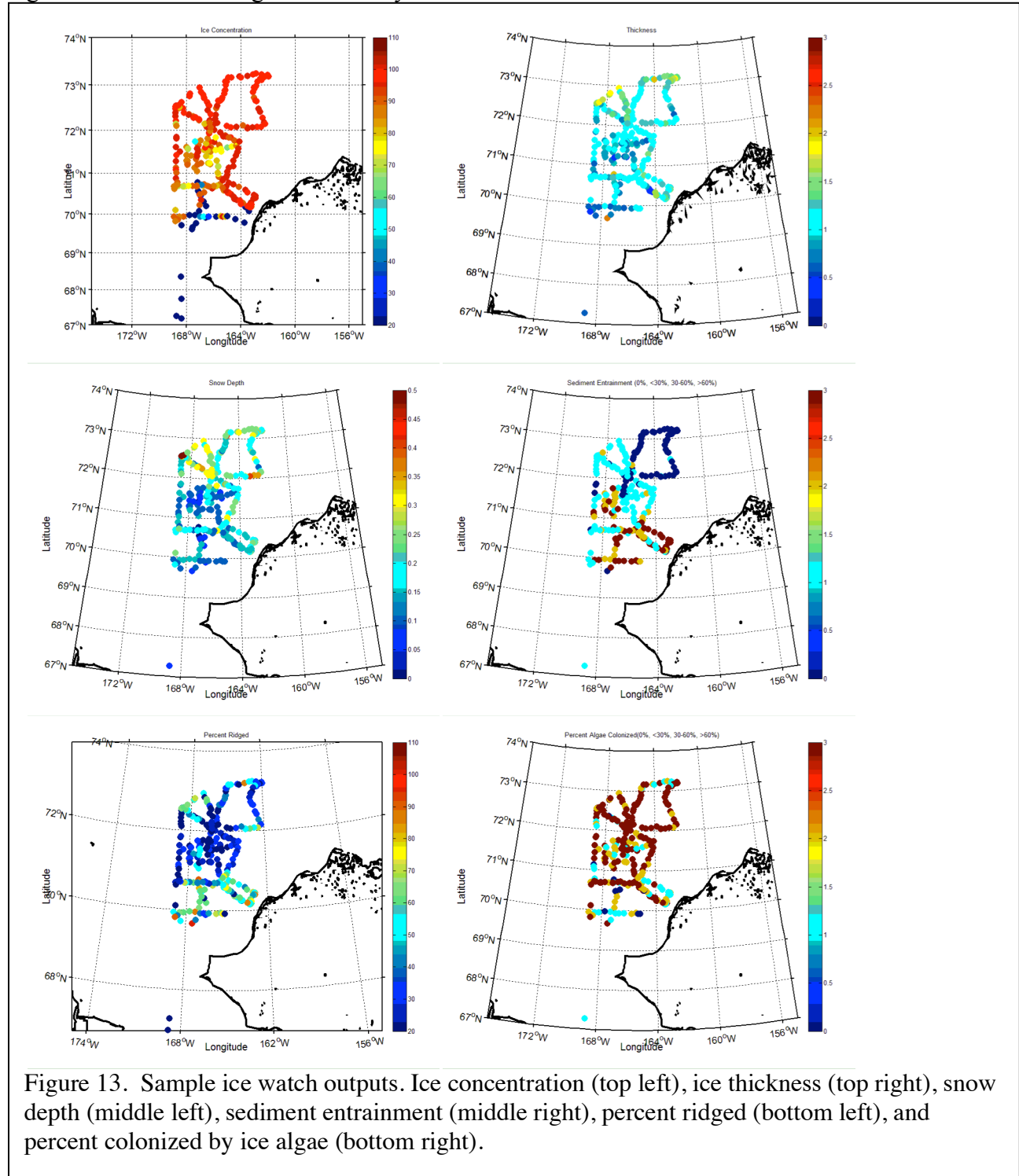


Figure 13. Sample ice watch outputs. Ice concentration (top left), ice thickness (top right), snow depth (middle left), sediment entrainment (middle right), percent ridged (bottom left), and percent colonized by ice algae (bottom right).

## Preliminary Conclusions

- Light transmission through ice into the upper ocean was low, partially due to a late melt onset and remaining snow cover throughout most of the cruise, but also due to large amounts of ice algae in place on the ice bottom.
- Onset of pond formation, while only observed in isolated cases, immediately lowered albedo from approximately 0.6 to 0.2 and increased transmission of visible light by a factor of 3.2.
- A late season snowfall and northerly winds appeared to combine to reset albedo to a higher level and delay melt onset compared to recent years.
- Thermodynamically formed first year ice thickness, which averaged 1.0 m in our preliminary processing, was relatively low compared to the 2010-2011 ICESCAPE mission. During the ICESCAPE missions, almost 1 month later in melt season, ice thickness was very similar or thicker. This is consistent with a very warm winter in the Alaskan Arctic, however sensor recalibrations will need to be applied prior to final conclusions on thickness change.
- Impact of the dynamic coast shore lead environment on the sea ice character was readily apparent. Ice watch results show that ice in the southern part of our operational area was more deformed, thinner (where undeformed), had less snow, and entrained more sediment.
- Permeability of all ice measured was 1-3 orders of magnitude too high to support melt pond formation above freeboard. Infiltration of fresh water from snow melt was observed to artificially seal the porespace in the sea ice, permitting the formation of above-sea-level ponds.

## Phytoplankton physiology and biogeochemistry

**Kevin Arrigo, Matt Mills, Kate Lowry, Kate Lewis, Ginny Selz, Hannah Joy-Warren,  
Caroline Ferguson, Erin Dillon**

*Stanford University*

**Joanie Ferland, Pierre Coupel**

*Takuvik Joint International Laboratory (CNRS-University Laval)*

**Jan Nash-Arrigo**

*Addison Elementary School*

### Objectives

The primary objective of the Phytoplankton physiology and biogeochemistry group during the 2014 SUBICE expedition was to characterize the biology of the pre-bloom phytoplankton community, and the oceanographic conditions that lead to under-ice phytoplankton blooms. We sampled the core biological variables (Table 1) at both the water column and ice stations. At multiple water column and ice stations the phytoplankton community was size fractionated (<20  $\mu\text{m}$  and total phytoplankton community) with the goal of better understanding the relationship between the ice algae and open phytoplankton water communities. Additionally, we also measured several phytoplankton photophysiology variables including photosynthesis vs. irradiance curves (P vs. E), simulated in-situ primary productivity,  $\text{NO}_3^-$  and  $\text{NH}_4^+$  uptake by phytoplankton, and measurements of phytoplankton active fluorescence using a fast repetition rate fluorometer. Finally, twelve four-day incubation experiments were conducted to study the effects of visible light and ultraviolet radiation (UVR) on phytoplankton growth, community composition, and physiology. The objective of these experiments was to determine the importance of attenuation of UVR by sea ice in supporting the extremely high growth rates of the under-ice bloom observed in the Chukchi Sea in 2011. Our hypothesis was that phytoplankton are able to grow more effectively in an under-ice environment by allocating fewer resources to protection from the harmful ultraviolet radiation found at the surface in open water. The collected data will provide the core measurements of phytoplankton biomass and physiology that will be combined with the chemical and physical measurements collected by other groups to provide a detailed picture of the biological oceanography and biogeochemistry of the Chukchi Sea during May and June of 2014.

### Methods

*Core water column measurements.* At the water column stations samples were collected from multiple depths using 30 L niskin bottles attached to the CTD rosette. The typical depths sampled were surface, 5 m, 10 m, 25 m, 50 m, 2 m above the bottom, and the depth of the subsurface chlorophyll maximum, if present. The water from each depth was collected into 20L coolers, subsampled and filtered onto GF/Fs for the quantification of chlorophyll *a* and other phytoplankton pigments, mycosporine-like amino acids (MAAs), particulate organic carbon, nitrogen, and phosphorus (POC, PON, POP) concentrations. Additionally, the maximum efficiency of photosystem II (Fv:Fm), absorption cross section of PSII ( $\sigma_{\text{PSII}}$ ), and electron turnover in PSII ( $\tau_{\text{PSII}}$ ) were measured using a fast repetition rate fluorometer (FRRf).

*$^{13}\text{CO}_2$  primary productivity,  $^{15}\text{N}$  uptake by phytoplankton, and  $^{15}\text{N}$  nitrification.* Simulated in-situ primary productivity and uptake of  $\text{NO}_3^-$  and  $\text{NH}_4^+$  were measured from the standard depths collected during the CTD casts. Briefly,  $\text{H}^{13}\text{CO}_3^-$ ,  $^{15}\text{NO}_3^-$  and  $^{15}\text{NH}_4^+$  were added to triplicate 500 ml bottles of collected seawater such that additions amounted to a ~5-10% increase in the ambient C and N pools. The bottles were then incubated in on deck incubators cooled with ambient seawater. After 24 h the bottles were filtered onto precombusted GF/F filters. The

samples were dried and will be analyzed for isotopic enrichment post cruise at Laval University. Additional 500 ml bottles (both clear and dark) were filled with surface, bottom, and 25 m water, spiked with  $^{15}\text{NH}_4^+$ , and incubated for 24 h in the on-deck incubators. At 8h intervals ~60 ml from each bottle was filtered through a  $0.2\ \mu\text{m}$  syringe filter and frozen for the measurement of  $^{15}\text{N}^{18}\text{O}_3$  to determine nitrification rates.

*P vs. E.* In the P vs. E method, seawater samples are incubated under a range of light levels to measure the photophysiology of natural phytoplankton. The P vs. E curves produced provide estimates of maximum photosynthetic rates, the light intensity to which phytoplankton are adapted, light limited rates of photosynthesis and photoinhibition parameters. During SUBICE, P vs. E was measured at 119 CTD casts at two depths, 19 ice stations (for sea-ice algae), 12 UV inhibition experiments, and 19 size fractionation studies summing in total 407 total P vs. E curves.

For each P vs. E curve, 45 ml of seawater sample was spiked with 25  $\mu\text{l}$  of radiolabelled bicarbonate ( $\text{H}^{14}\text{CO}_3$ ). 2 ml of sample was added to 20 ml scintillation vials which were incubated in a photosynthetron for 2 hours at  $0^\circ\text{C}$  under a gradient of 14 light levels, ranging from approximately  $0.8$  to  $500\ \mu\text{Ein m}^2\ \text{s}^{-1}$ . Three vials were acidified immediately to provide the baseline  $^{14}\text{C}$  present. 100  $\mu\text{l}$  of sample was added to 70  $\mu\text{l}$  ethanolamine, 500  $\mu\text{l}$  filtered seawater and 5ml scintillation cocktail as a measure of how much  $^{14}\text{C}$  was present in total after spiking the sample. After the incubation, 250  $\mu\text{L}$  of 6 N HCl was added and allowed to vent for 24 hours to drive off unincorporated inorganic carbon. After neutralization with 250  $\mu\text{L}$  6 N sodium hydroxide, 10 mL of scintillation cocktail (Ecolume) was added and vials were tightly capped, shaken and packed. Because the liquid scintillation counter aboard broke irreparably within the first week of the cruise, the samples will be shipped back to Stanford University for analysis.

*UVR experiments.* Surface water was collected from the CTD rosette, screened for grazers with  $100\ \mu\text{m}$  Nitex mesh, and placed in UV-transparent Whirlpak bags (with a volume ranging from 3-5 L) for on-deck incubation using a seawater flow-through system. There were five different treatments, each with a different combination of visible light (high and low) and UVR exposure (high, low, and none). Each treatment contained a set of triplicate bags. The control was the high light and high UVR treatment. Light treatments were created using mesh screening and UVR-absorbing plexiglass (OP3-Acrylite). Each experiment was incubated on deck for a total of 96 hours with additional sampling time points at 0, 24, 48, and 72 hours.

At the initial (T0) and final (T96) time points, water was sampled for nutrient concentrations, chlorophyll *a* concentration, particulate organic carbon and nitrogen concentrations, phytoplankton pigments via HPLC, MAAs via HPLC, phytoplankton and detrital absorption (Ap/Ad), active fluorescence via FRR/f, and photosynthesis versus light (PvE) curves, using methods described in other sections of the cruise report. Additionally, water was sampled for FRR/F physiology at each daily time point and for nutrient and chlorophyll *a* concentrations at the experiment midpoint (T48).

*Ice stations.* We sampled at 16 ice stations during the cruise. At each station, multiple ice cores were taken and sectioned at 10 cm intervals. One ice core was melted and sampled for the measurement of nutrient ( $\text{NH}_4^+$ ,  $\text{NO}_3^-$ ,  $\text{PO}_4^{3-}$ , Si) concentrations and salinity. A second core was used to quantify biomass throughout. Briefly, each section was melted in 2 L of  $0.2\ \mu\text{m}$  filtered seawater (FSW) and then subsampled and processed for measurements of chl *a* concentrations and POC/N/P concentrations. The bottom 10 cm of a third core was melted in  $0.2\ \mu\text{m}$  FSW and subsampled for measuring pigment and MAA concentrations using HPLC, active fluorescence using FRRf, and P vs. E light curves.

*Size fractionation.* Motivated by previous research suggesting small ice algae may “seed” the water column, samples from ice and water column stations were further size fractionated into a total and  $<20\ \mu\text{m}$  fraction before analysis. At each ice station and two open water stations (19

stations total), we size-fractionated two depths (surface and subsurface chlorophyll maximum or 25 m. when the subsurface chlorophyll maximum was absent). Samples were collected for chl *a*, HPLC pigment composition and concentrations, MAA concentration (surface depth only), POC/N/P, FRRf, and P vs. E. To separate out the small fraction (<20 µm) samples were gravity filtered through 20 µm nitex mesh.

### **Preliminary findings**

The majority of our results will come after the cruise. All particulate organic and HPLC samples must be prepped and analyzed at Stanford University. Additionally, all stable and radioactive isotope and molecular samples collected will be analyzed over the next 6-12 months at Stanford University. At this point our preliminary findings indicate that the early season (pre-spring bloom) phytoplankton community below the ice is low in concentration, and while photosynthetically active, has a low maximum efficiency of PSII (Fv:Fm 0.3 or less). The low Fv:Fm can indicate a phytoplankton community in stress, though may also indicate a different community (e.g. picophytoplankton or cyanobacteria) than the one that eventually blooms once enough light is present (i.e. diatoms such as *Chaetoceros* sp. or *Fragilariopsis* sp.) The HPLC pigment analysis combined with the imaging flow cytobot (Babin, Laval and Laney, WHOI and flow cytometry (Laney, WHOI) cell counts will help elucidate these differences.

Currently, the available data from the UV experiments include chlorophyll *a* concentrations, nutrient concentrations, phytoplankton and detrital absorption, and FRR/F physiology parameters including Fv/Fm, Fo, Fm, Sigma, and TauQA1. Data from the experiments indicate that phytoplankton in the low or no UVR treatments had higher chlorophyll *a* concentrations and nutrient deficits and were generally more efficient than phytoplankton in the high UV treatment. However, more sample and data analysis is needed before conclusive results will be available.

## **Radiosondes (Weather balloons) and Ceilometer (Cloud Height measurement)**

**Sigrid Salo**  
*NOAA/PMEL*

### **Objectives**

Pacific Marine Environmental Laboratory, a National Oceanic and Atmospheric Administration laboratory, sent one person (Sigrid Salo) on the cruise to do atmospheric soundings and to measure cloud height. The goal of the project was to add to the knowledge of atmospheric conditions within the springtime ice pack in the Chukchi Sea by sampling as wide a geographic range of locations and ice concentrations as possible under a variety of wind conditions. In addition, most of the soundings were carried out at 00GMT and 12GMT (when weather stations also launch balloons) in order to compare our results with onshore soundings at Barrow, to assess how closely Barrow readings describe offshore conditions and to obtain some regional scope to our data.

### **Methods**

We launched 80 radiosondes during the cruise at times and locations listed in the table attached to this report. We used Vaisala RS92 radiosondes and a Vaisala DigiCORA MW-41 sounding system to set up and track the radiosondes. The radiosondes measure pressure, air temperature, humidity and GPS position (from which the MW-41 system calculates winds) and send the data back to the MW-41 system via UHF. Most radiosondes rose higher than 20,000 m before the balloons burst; depending on wind speeds and directions they were generally 15-40 km from the ship at that point.

Boundary layer and cloud height were measured with a Vaisala CT31 ceilometer using Vaisala's BLView software. The ceilometer is a laser instrument that uses the strength and timing of the return-signal from the laser to calculate cloud height and density. BLView also calculates estimates of the atmospheric boundary level height. The ceilometer was set up on the aft 04 deck and ran continuously throughout the cruise.

### **Preliminary Findings**

As we hoped, we were able to sample a wide range of ice conditions and locations under a variety of wind directions, although most wind speeds were low - less than  $10 \text{ m s}^{-1}$ , and often about half that speed. In addition, we were able to obtain ceilometer data for conditions ranging from quite dense fog or stratus clouds to clear skies. However, we have to carry out quite a bit of further processing and comparisons to derive any conclusions from our findings.

## **Application of Ra isotopes and trace metals to study the role of iron (Fe) in the formation of large phytoplankton blooms under the ice in the Arctic Ocean**

**Lucia Helena Vieira and Joaquin Pampin Baro**  
*Helmholtz-Zentrum für Ozeanforschung Kiel - GEOMAR*

### **Objectives**

Iron is an essential micronutrient for living organisms and plays an important role in plankton productivity in the ocean. Thus, scientists have studied the biogeochemistry of Fe in the oceans in more detail to understand the relationship between Fe supply and microbial productivity and ecosystem structure. However, the debate about Fe limitation of phytoplankton in the ocean has highlighted how little we know about the marine biogeochemistry of Fe, its distribution in the ocean and its intrinsic relationship with biota.

In this context, natural radionuclides may be used as tracers to investigate the possible input sources of Fe in the ocean. Their applications in oceanography elucidate the processes occurring in the water column (particle transport, carbon cycle, biogeochemical cycles, and scavenging processes) or sediments (sinking, deposition, accumulation, transportation and resuspension). Radium isotopes, for example, are excellent tracers of sources of Fe in the region of interest of this study.

Therefore, the issues of this current research project are centered on the variability of supply of Fe and how it regulates the spatial and temporal distributions of phytoplankton communities, the structure of the plankton community and its ecology. Thus, the aim of this research work is to study the role of Fe in the formation of large phytoplankton blooms that occur beneath the sea ice in the Arctic Ocean. In addition to Fe, we will study a range of trace metals, including Mn, Cu, Co, Zn, Ni, Al, Pb, Cd, which act as micronutrients for phytoplankton (Mn, Cu, Co, Zn, Ni, Cd) or tracers of ocean processes (Mn, Al, Pb, Cd). The availability of these elements in the study area will be evaluated to trace possible sources of Fe and determine the Fe source strength. Besides, the natural Ra isotopes (Ra-223, Ra-224, Ra-226 and Ra-228) will be used as tracers of mixing rates of water masses and they can also outline the sources of iron to the system.

### **Methods**

In this research, cruise samples were collected for trace metals, DIC,  $^{18}\text{O}$ , and radium analysis.

#### **Trace Metals sampling**

For sampling the seawater in metal free conditions, we used PVC hose, previously washed with DECON for 3 days and acid washed for 1 week with HCl 10%vv to avoid leaching contamination inside the walls of the hose. This was attached alongside a coated wire with marks every 5 meters, with a 25 kg coated weight attached at the end. Water was pumped onboard the ship using a Teflon Pump (ALMATEC) driven by compressed air to feed the pump.

A container placed on deck was made trace metal clean. Working areas were wrapped with clean plastic film to avoid metal contamination, air currents and dust in the sampling areas. Water was pumped directly into the container.

While sailing in open water, a towed fish has been deployed to collect surface seawater in the transect between Dutch Harbor and the Bering Strait.

**Sampling procedure.** A hose/wire was manually deployed off the starboard side preferentially, at the depths of 15, 25, 35, and 45m. The deepest station sampled was 70 m. No water was sampled between the surface and 15 m due to the ship's hull, that reaches 8 m deep into the water column.

The hose was flushed at every depth for approximately 7 min, in order to run 6 L of seawater from the specific depth we were sampling to guarantee we sampled the desired depth.

Before every station, diluted HCl (5% vv - prepared in MQ water) was run through the hose to avoid memory effect from previous stations.

Samples were taken in LDPE bottles 125 mL, specially washed in clean conditions, through different baths, for 1 week in each: DECON, HCl 30%vv, and HNO<sub>3</sub> 50%vv to remove metal leaching, and several times rinsed with MQ ultrapure.

The order for sampling was 1) Ligands, Unfiltered in 250mL LDPE bottles, 2) unfiltered samples for Total dissolvable (Particulated+dissolved) Metals: in 125mL LDPE, and 3) filtered samples with Sartorius accropack 0.8-0.4um for Dissolved Metals, in 125mL LDPE.

Sample treatment. Ligands were directly placed into the freezer after sampled. Trace metals samples were acidified within a Laminar Flow Hood with HEPA filters class 100, with 150 uL of HCl OPTIMA grade from Fisher (less than 5 ppt impurities) to reach pH ~2.

No analysis for trace metals was carried out on board. Trace metals will be determined by Flow Injection Chemiluminescence (FIA) and Isotope Dilution - Inductively Coupled Plasma Mass Spectrometry (ID-ICPMS). The samples will be first analyzed by FIA to measure Fe as approach the metal concentrations, and then by isotope dilution and online preconcentration by SeaFast with ICP-MS Elemental II, to determine Fe, Zn, Cu, Ni, Co, Mn, Pb, and Al. We do not discard the possibility of making dilutions of the samples for analysis of Total Dissolvable Fe (Particulate-Unfiltered).

### Radium sampling

On ice stations, seawater from 10 m depth was sampled from the CTD cast. A 200 L barrel was filled with seawater which was slowly filtered (around 1 L/min) through a cartridge filled with MnO<sub>2</sub>-impregnated acrylic fiber (Mn-fiber). After that, the fiber was washed with Ra-free water or Milli-Q water and dried in order to be measured on the Radium Delayed Coincidence Counter (RaDeCC).

On normal water stations, science seawater was collected. With a hose connected to the tap, the barrel was filled up with the science seawater. After that, the same proceeding described above is carried out. Between Dutch Harbor and the Bering Strait, three samples were taken using the Tow Fish.

The process of pumping from the barrel to the cartridge with the Mn-fibers, and of washing and drying the fibers, takes about 4.5 h. For that reason, it was not possible to sample all the water stations.

The short-lived radium isotopes (Ra-223 and Ra-224) were counted on board on a Radium Delayed Coincidence Counter (RaDeCC). However the concentrations of those elements will be analyzed and processed on land. For now, we have only the number of counts.

The same fibers used to measure short-lived isotopes will be used to measure long-lived radium isotopes. Thus, determination of Ra-226 and Ra-228 activity will be performed by measuring the gross-alpha and beta activity of the Ba(Ra)SO<sub>4</sub> precipitate using a low-background gas-flow proportional counter. This technique is advantageous because it presents a low background radiation.

### Expected Results

The sources and sinks of Fe will be elucidated and quantified. We will use tracers of atmospheric inputs (Al) to quantify inputs, and vertical diffusive fluxes of Fe and other elements will be determined as well.

Sediment supply and subsequent lateral transport will be determined using the Ra isotopes tracers. In addition, Mn will be used as a tracer for reductive benthic supply. The sources of other

biogenic trace elements will be used to assess the potential or potential co-limitation of primary productivity by these elements. Previous studies and publications about this currently study area show high concentrations of Fe particulate and lower concentrations of dissolved Fe fraction. Although we might say these studies have been undertaken mainly in summer time when Fe and other elements concentrations may change after the occurrence of the phytoplankton bloom.

## **Imaging Flow Cytobot I**

**Dean Stockwell**

*University of Alaska Fairbanks*

**Sam Laney**

*Woods Hole Oceanographic Institution*

One of the primary goals of this component was to operate the Imaging FlowCytobot in flow-through mode on the transit up to and back from the Chukchi study region, and throughout the study region between fixed stations, using an ad-hoc surface seawater supply located in the fueling hose room, 2<sup>nd</sup> deck. The phytoplankton cell images collected with this instrument provide information about the microplankton assemblage composition, for comparison to HPLC proxies for assemblage composition and for direct assessment of algal composition while at sea. A secondary goal was to use the same instrument (together with a second instrument operated by the Takuvik group, see below) to examine discrete volume samples, e.g. from CTD casts (Niskin samples), from ice stations (meltponds, sub-ice profiles, and melted sea ice). For most CTD stations, the same seawater samples were analyzed using flow cytometry (FCM) on ship, with an Accuri C6 flow cytometer. During the flow-through sampling periods, periodic samples with also run on the Accuri C6 flow cytometer.

Samples from CTD bottles were analyzed from 126 of the 230 CTD stations occupied during HLY 1401. The stations that were skipped corresponded primarily to many of the “chlorophyll-only” stations on closely spaced transects, where no time was available to perform IFCB analyses. Between-station sampling in flow-through mode was performed over approximately 2800 nm in HLY 2014. Underway collection of images across the Bering Sea were collected both leaving from and returning to Dutch Harbor.

### **Preliminary Findings**

Results will be analyzed after samples are returned to home institution for analysis.

## Imaging FlowCytobot II

Joannie Ferland and Marcel Babin

*Takuvik Joint International Laboratory (CNRS-University Laval)*

### Objectives

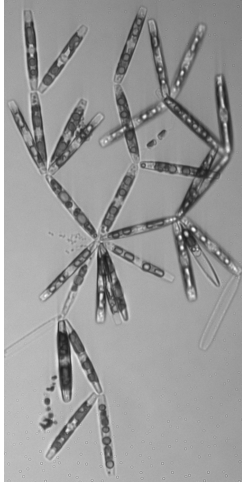
The main goal of the Imaging Flowcytobot (IFCB) measurements is to better characterize the nano- and microplankton (2-150  $\mu\text{m}$ ) community of the different arctic habitats surveyed: ice free water column, sub-ice water, ice sheet, melt pond. The novel contribution of the IFCB is to allow direct and detailed assessment of phytoplankton composition while at sea.

Specific objectives were to identify and quantify the succession of dominating species of phytoplankton under the ice and at the ice marginal zone.

### Methods

Samples from 679 CTD bottles were analyzed from 157 of the 230 CTD stations during the Healy 1401 SUBICE expedition. In addition, 123 ice core samples (including 10 complete cores layered by 10 cm), 16 sub-ice water samples and 3 melt ponds samples were analyzed from the 15 ice stations studied.

Two IFCBs were running samples in size fraction complementarity as Sam Laney's IFCB had an entrance mesh of 300  $\mu\text{m}$  compared to 150  $\mu\text{m}$  for the IFCB-Takuvik. Also, Dean Stockwell ran Sam Laney's IFCB underway, sampling via the flow through system at the end of the expedition as the IFCB-Takuvik kept running discrete sampling from CTD bottles, ice core, melt pond and sub ice. The setting of the instrument was also slightly different, giving the idea that the IFCB-Takuvik captured a bigger proportion of the smaller cells. The two datasets shall be closely analysed as to get the most accurate understanding of the algae structure observed during this SUBICE expedition.



### Preliminary Findings

The dominant species of ice algae communities (Figure 1) forming dense mat at the bottom of the ice differed significantly, but not surprisingly, from the phytoplankton water column communities (Figure 2) wherever stations were sampled in the Chukchi Sea.

Figure 1. Different species of ice algae.

### Conclusions

The dataset will be post-cruise analyses by Pierre-Luc Grondin as a master degree project co-supervised by Marcel Babin at Laval University and Lee Karp-Boss at University of Maine. The study will address a more detailed examination of vertical and horizontal distribution of the plankton structure.

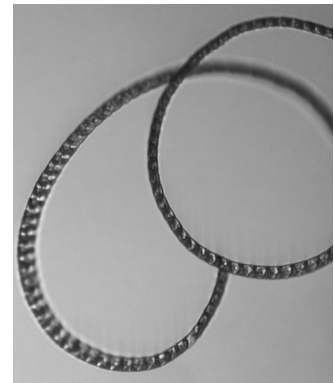


Figure 2. Different species of water column phytoplankton.

## Nutrient assimilation and regeneration ( $^{15}\text{N}$ and $^{13}\text{C}$ Incubations)

Pierre Coupel and Jean-Eric Tremblay

*Takuvik Joint International Laboratory (CNRS-University Laval)*

### Objectives

Determine the nutrient assimilation and regeneration before the productive season when the Chukchi Sea is ice covered and potentially during an under-ice bloom.

### Methods

$^{15}\text{N}$  –  $^{13}\text{C}$  Incubations. Incubation experiment were conducted to determine the assimilation and regeneration of  $\text{NO}_3$ ,  $\text{NH}_4$  and C. Water samples were incubated in deck incubators during 24 h in 500 ml polycarbonate bottles after  $^{15}\text{N}$  –  $^{13}\text{C}$  stable isotopes addition. The amount of stable isotopes added was kept low (less than 10% of the ambient concentration) to avoid artificial stimulation of the phytoplankton. To reproduce the light availability at the different depths sampled (4-5 depths), the incubated bottles were placed in bags covered by mesh grid layers. A cover absorbing 75% of the incident light was placed on the incubator to simulate the light attenuation by the ice cover. Temperature in incubators was maintained by pumping water from surface ocean using tubes.

The incubation bottles were filtered after 24 h. The material collected on filters will be analyzed by mass spectrometry back in University Laval to assess the assimilation of stable isotopes in the particulate pool. The filtrates were poisoned and store in dark bottles at room temperature until analyses to determine the regeneration of  $\text{NH}_4$  by bacteria. During the same incubation experiment, samples were taken every 8h to determine the nitrification. These data will be analyzed and interpreted by Matt Mills from Stanford University.

### Nutrients utilization

Moreover, concentrations of  $\text{NO}_2$ ,  $\text{NO}_3$ ,  $\text{NH}_4$ ,  $\text{PO}_4$  and  $\text{SiO}_4$  were measured at the beginning (T0h) and the end of incubation (T24h) from sub-samples of the incubation bottles. The difference in nutrient concentration between T0h and T24h provide a direct estimate of the nutrient consumption. Dan Schuller from Scripps University measured the T0h and T24h nutrient concentrations onboard with an Auto-Analyzer.

Intracellular nutrient content. The intracellular nutrient contents were measured at stations where incubations were done. For each depth, 1 L of seawater were filtered on pre-combusted filter. After filtration, boiled water was added onto the filter to burst the cells and collect their intracellular nutrient content. The nutrient concentration in the filtrates was measured onboard with an Auto-Analyzer (Dan Schuller from Scripps Institution of Oceanography).

### Preliminary Findings

Low nutrient uptake rates were observed at most of the stations ( $\text{NO}_3 = 0$  to  $0.5 \mu\text{M L}^{-1} \text{d}^{-1}$ , Fig.1). The uptake of nutrients being inhibited by the low light resulting from thick ice covers and ice algae shading. Due to low phytoplankton biomass and nutrient uptake, low intracellular nutrient concentrations were observed especially for the nitrate in deficit compared to phosphate and silicate.

The nutrient uptake increases ( $\text{NO}_3 = 1$  to  $4 \mu\text{M L}^{-1} \text{d}^{-1}$ ) in the few coastal stations where open water was encountered. These highest uptakes are related with high chlorophyll concentration ( $\text{Chl } a > 1 \text{ mg m}^{-3}$ ). In stations with high chlorophyll concentration and high uptake, the phytoplankton seems to overtake the nitrate (N/P uptake = 20, N/Si uptake = 2) in comparison to the nutrient proportion observed in the water column (N/P = 7 and N/Si = 0.3). The high uptakes of nitrate observed in the high chlorophyll station are associated to elevated

intracellular nitrate concentration resulting in high intracellular N/P and N/Si ratios.

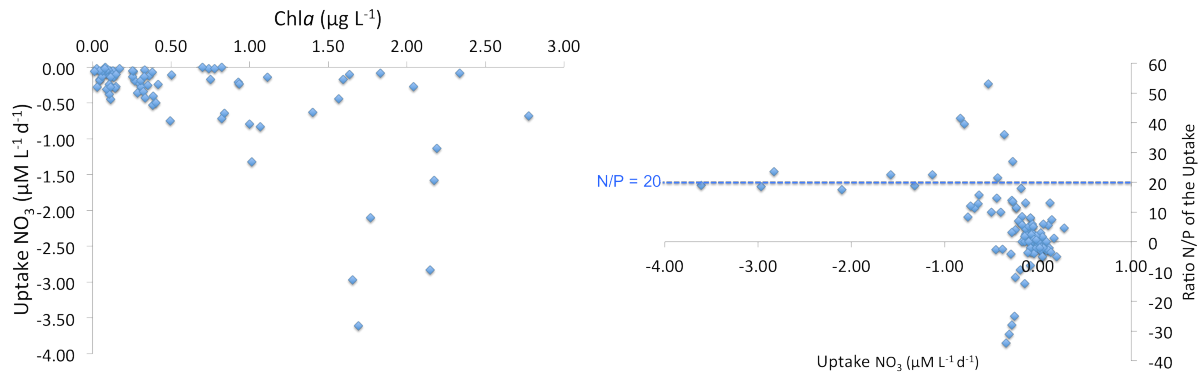


Figure 1. (left graph) Relationship between the chlorophyll-a concentration and the uptake of nitrate. (right graph). Relationship between the uptake of nitrate and the N/P ratio of the phytoplankton uptake. The ratio N/P observed in the stations with a high uptake is mentioned on the graph with the dotted blue line.

### Preliminary **Conclusions**

Under the ice cover, we observed a system with high nutrients and low phytoplankton chlorophyll biomass, resulting in slow phytoplankton activities limited by the light availability. The microbial role on nutrient regeneration and transformation should be important. Future analyses of <sup>15</sup>N and <sup>13</sup>C will provide more information about the precise uptake and primary production by phytoplankton and regeneration by bacteria of the nitrogen.

## Prokaryotic abundance and production, dissolved organic matter

Guillaume Meisterhans, Christine Michel

*Marine productivity laboratory - Freshwater Institute  
Fisheries and Ocean Canada, Winnipeg*

### Objectives

The ocean is the main organic carbon reservoir with more than 95% of total carbon on Earth (Watson and Orr, 2003). Part of the available fraction of this organic matter is assimilated by prokaryotes (Robinson and Williams, 2005). Therefore, prokaryotes play a key role in the ecosystem recycling the organic matter in mineral matter that becomes available for primary producers.

Our study aims to estimate the concentration in dissolved organic matter (DOC and DON) and the abundance and the production of the prokaryote community in water, sea-ice and melt pond in winter/spring condition during (i) the period when the water mass is characterized by high concentrations in nutrients, (ii) the melt ponds formation and (iii) the formation of the under-ice phytoplankton bloom as previously reported in this area (ICESCAPE 2011)

### Methods

From May 16<sup>th</sup> to June 19<sup>th</sup> 2014, 121 stations were sampled as summarized in the Table 1. All stations were sampled for prokaryotic abundance and production. Only 107 of the 120 CTD water stations were sampled for DOC/DON.

Table 1. Summary of sampling done during SUBICE 2014

	N station	DOC / DON	Prokaryote abundance	Prokaryote production
Seawater	120	502	1751	2945
Bottom Ice core	19	38	57	95
Top ice core	10	20	30	50
Melt pond water	2	6	9	15
Total		566	1847	3105

Sea-ice cores were collected using a manual ice corer (Mark II coring system, 9 cm internal diameter, Kovacs Enterprises). Cores were cut to collect the bottom 3 cm and the 10 top cm ice sections only and each section was stored in a sterile Whirlpak bag. Ice core

sections were stored in the dark at room temperature (ca. 15°C) allowing ice to melt slowly overnight.

Surface seawater was collected at 4 to 9 different depths (Table 2), depending of both the maximal depth and the preliminary CTD data. Samples were taken directly from the Niskin bottle spigot using a 60 mL syringe for dissolved organic matter and prokaryote abundance and in clean 20 mL scintillation vials previously rinsed 3 times with the sample for prokaryote production

Melt pond water was collected in 125 mL Nalgene bottle previously rinsed 3 times with the sample. Dissolved organic matter, prokaryote abundance and prokaryote production were measured on each sample. 20 or 40 mL duplicate subsamples were filtered through pre-combusted (450°C for 5 h) Whatman GF/F filters (nominal pore size of 0.7 µm) and stored in the

dark at 4°C after being acidified with phosphoric acid (5% final concentration, Sigma) until determination of DOC and DON concentrations using high-temperature catalytic combustion on a Shimadzu TOC-VCPH analyzer coupled with a TNM-1 Total Nitrogen module (Knap et al. 1996). Triplicate 4 mL subsamples were fixed with glutaraldehyde Grade I (0.5% final concentration; Sigma) and frozen at -80°C for later determination of the prokaryote abundance by flow cytometry according to Belzile et al. (2008).

Triplicate 1.2 mL subsamples were spiked with 3H-leucine (specific activity, 60 Ci mmol<sup>-1</sup>) at a final concentration of 10 nM and incubate 2 hours at *in situ* temperature to measure the prokaryote production according to Knap et al. (1996). Incubations were stopped by adding TCA (5% final concentration) and samples were stored at -80°C until analysis. In addition, two controls were simultaneously conducted to determine background level by adding trichloroacetic acid (TCA, 5% final concentration) to the 1.2 mL samples prior to the incubation in order to kill prokaryotes. Back at the Freshwater Institute facilities, samples will be gently thawed at 4°C then centrifuged (14000 rpm, 10 min) to pellet the prokaryote cells and remove supernatant. The precipitate was rinsed once with 5% TCA. TCA will be eliminated by a second centrifuge step (14000 rpm, 10 min). The precipitates will be resuspended in 1.5 ml of liquid scintillation cocktail (Ecolume, MPBio) and radioactivity will be measured using a liquid scintillation counter (PerkinElmer). Data will be given in pmol of leucine incorporated per liter and per hour (pmol Leu L<sup>-1</sup> h<sup>-1</sup>) and also converted in g C L<sup>-1</sup> h<sup>-1</sup> using the conversion factor of 3.1 kg C mol<sup>-1</sup> of 3H-leucine (Kirchman and Ducklow 1993).

### **Preliminary Findings**

Results will be analyzed after samples are returned to home institution for analysis.

## **Microbial community composition and viral production**

Chiaki Motegi and Connie Lovejoy  
*Takuvik Joint International Laboratory (CNRS-University Laval)*

### **Objectives**

To determine microbial diversity, community composition and abundance, and viral production in the water column, bottom ice and beneath the ice in the Chukchi Sea.

### **Methods**

Microbial DNA and RNA samples were collected and will be determined by pyrosequencing in a land laboratory. Abundance of eukaryotes and prokaryotes and its phylogenetic group will be determined by DAPI count (Porter & Feig 1980) and fluorescent in situ hybridization (FISH, Amann et al. 1995). Viral production rates were measured using the reduction approach (Weinbauer et al. 2010).

Microbial DNA and RNA. Six L of 50- $\mu\text{m}$  pre-filtered seawater sample was filtered through a 3- $\mu\text{m}$  polycarbonate filter and then through a 0.22- $\mu\text{m}$  Sterivex filter to collect eukaryotes and prokaryotes DNA and RNA. Filters were stored at  $-80^{\circ}\text{C}$  in a buffer solution. For viral community, 1 L of filtrate ( $<0.22\mu\text{m}$ ) was concentrated with 100 kDa cartridge (final volume 25 mL, Vivaflow200) and stored concentrates at  $-80^{\circ}\text{C}$ . Samples will be measured in a land laboratory.

DAPI counts. Samples for eukaryote and prokaryote abundance were preserved with glutaraldehyde solution (final concentration 1%). Samples were stained with 40-6-diamino-2-phenylindol (DAPI, final concentration  $5\ \mu\text{g ml}^{-1}$ ) for 5 minutes, and filtered through a 3- $\mu\text{m}$  and a 0.2- $\mu\text{m}$  polycarbonate black filter to collect eukaryotes and prokaryotes. Filters were mounted onto glass slides with a drop of immersion oil and stored in the dark at  $-20^{\circ}\text{C}$ . Eukaryotes and prokaryotes abundance will be determined by epifluorescence microscope in a land laboratory.

Fluorescent in situ hybridization (FISH). Sample for abundance of eukaryote and prokaryote phylogenetic groups were preserved with paraformaldehyde solution (final concentration 2.2%). After fixation at  $4^{\circ}\text{C}$  for 6 h, samples were filtered through a 3- $\mu\text{m}$  and a 0.2- $\mu\text{m}$  polycarbonate filter to collect eukaryotes and prokaryotes. Filters were stored at  $-20^{\circ}\text{C}$  and phylogenetic group abundance will be determined by fluorescent in situ hybridization in a land laboratory.

Viral production. One L water samples were concentrated using a 0.2- $\mu\text{m}$  polyethersulfone membrane cartridge (Vivaflow50) to collect bacteria. The filtrate was passed through a 100 kDa cut-off membrane (Vivaflow200) to produce virus-free seawater. Three mL of the bacterial concentrates were added to 50 mL of viral-free water. The virus-reduced culture was incubated in a 50 mL conical tube at in situ temperature in the dark, and subsamples for counting viruses were withdrawn at 3 h intervals until the end of the 12 h incubation period. Subsamples for counting viruses were collected in 2 mL cryovials, preserved with glutaraldehyde (final concentration 0.5%) and stored at  $-80^{\circ}\text{C}$  (directly or after having been deep frozen in liquid nitrogen). Viral abundance will be determined by flow cytometry in a land laboratory.

### **Preliminary Findings**

Results will be analyzed after samples are returned to home institution for analysis.

Table 1. Summary of data collected during SUBICE 2014

Parameter	Number of samples		
	Water	Bottom ice	Beneath the ice
3-50 $\mu$ m	44	15	9
Diversity 0.2-3 $\mu$ m	44	15	9
100kDa-0.2 $\mu$ m	4		
DAPI	35	9	7
FISH	35	9	7
Viral production	7		

## Biomarkers

Caroline Guilmette and Guillaume Masse  
*Takuvik Joint International Laboratory (CNRS-University Laval)*

### Objectives

The main objective was to identify and quantify the main lipids present in both sympagic and planktonic algal communities. The carbon isotopic composition of the main lipids will be determined in an attempt to obtain diagnostic values to discriminate between the sources. We also measured several associated biological and chemical variables to better understand the distribution of the studied biomarkers.

### Methods

At each ice station, samples were collected at 10 m depth or SCM when observed with the CTD-Rosette, 1 m under the ice floe with a submersible pump, and the bottom 10 cm ice core diluted with 0.2 µm filtered sub-ice water

Lipids isotope and concentration. For each sample, a minimum of 3 L of seawater was filtered on Whatman GF/F glass fiber filters for determination of IP<sub>25</sub> presence/absence and carbon isotopic ratios. Samples were stored at -80°C until laboratory analysis on a GC-IRMS Thermo Delta V Plus at Laval university. Additional phyto and zooplankton samples were collected for the same measurements following the listed protocols.

Zooplankton biomarkers. For each station, several top to bottom net deployments under the ice were accomplished using a 150 µm mesh. One or more aliquots of 100 mL were fixed using 10% formaldehyde as to identify the zooplankton community prior to lipid analysis.

Phytoplankton biomarkers. For each station, several top to bottom net deployments under the ice were accomplished using a 20µm mesh. The phytoplankton samples were re-filtered on a 150µm mesh in the wet lab to remove the zooplankton fraction. This fraction was added to the zooplankton samples. The phytoplankton fraction was then centrifuged for additional concentration of the biomass. The samples were stored at -80°C until analysis at Laval University.

Particulate carbon. For each sample, 500 ml to 2L of seawater was filtered on pre-combusted Whatman GF/F 25mm glass fiber filter for the determination of isotopic ratio <sup>13</sup>C/<sup>12</sup>C. Samples were dried in the oven at 60°C and kept dried in the dark until laboratory analysis will be performed. Analysis will be done on an EA-IRMS Thermo at Laval University.

Biogenic silica: For each sample, 500 ml to 1L of seawater was filtered for determination of biogenic silica concentration. Filters were stored at -80°C until laboratory analysis at Laval University.

Particulate DMSP (DMSPp). For each sample, 1-2 L of seawater was filtered on Whatman GF/F and acidified with 2 mL of 10% H<sub>2</sub>SO<sub>4</sub> for the determination DMSPp concentration. Filters were stored at -80°C until laboratory analysis on a GC at Laval University.

Pigments (HPLC). For each sample, 500 mL to 1 L of seawater was filtered on Whatman GF/F for the determination of phytoplankton pigment concentration (HPLC). Filters were stored at -80°C until laboratory analysis at Laval University.

Chlorophyll *a*. For each sample, 25 to 500mL of seawater was filtered on Whatman GF/F 25 mm. Extraction with 90% acetone and fluorimetric measurements were performed by Kevin Arrigo's team on board using a Turner-Design Model 10AU fluorometer.

Phytoplankton identification and abundance. For each sample, 20 ml and 225 ml were collected respectively from the ice core and, sub-ice and water column, for phytoplankton

identification and abundance. Samples were fixed with acidic Lugols solution and stored at 4°C until analysis. Taxonomic analysis will be performed using inverted microscopy upon arrival of samples at Laval University.

Imaging Flowcytobot (IFCB): For each samples, 60 mL were collected for simultaneous taxonomy identification by Joannie Ferland using the Image Flowcytobot of the Takuvik team. The instrument was set to screen organisms smaller than 150 µm.

Nutrients. For each sample, 30 mL of water was sampled and filtered on Whatman GF/F 25mm for nutrients. Analysis was performed on board on an autoanalyser III by Dan Schuller.

Table 1. Summary of data collected during SUBICE 2014

Parameter	Water 10m	SUBICE	Bottom Ice	Melt Pond	Plankton
Lipids	14	15	15	2	15
Particulate Carbon	14	15	15	2	
DMSP	14	15	15	2	
Biogenic Silica	14	15	15	2	
Pigments HPLC	14	15	15	2	
Taxonomy	14	15	15	2	
Chlorophyll <i>a</i>		15	15	2	
Nutriments		15	15	2	
IFCB		15	15	2	

## Herbivory and Bacterivory Rate Measurements

Paige Connell

*University of Southern California*

### Objectives

The goal of this study was to characterize the protistan grazer community, both nanoplankton and microzooplankton, and the grazing mortality of the phytoplankton and bacteria at different stages of the spring/summer bloom in the Chukchi Sea.

Specifically, I aim to characterize the following aspects throughout the seasonal evolution of the bloom, 1) The community composition and biomass distribution of the predator (grazer) and prey (phytoplankton) communities, 2) the growth and grazing mortality of the phytoplankton community, and 3) the grazing mortality of the bacterial community

### Methods

**Microscopy.** To enumerate the microplankton, both large phytoplankton and microzooplankton, preserved seawater will be enumerated in settling chambers on an inverted microscope (Utermohl 1958). The nanoplankton community, as well as the trophic status (heterotrophic vs. phototrophic/mixotrophic) of microzooplankton grazers, will be characterized through epifluorescent microscopy of prepared DAPI slides.

**Size-fractionated Chlorophyll.** Initial phytoplankton community composition was also assessed through size-fractionated chl *a* measurements for the <200  $\mu\text{m}$ , <20  $\mu\text{m}$ , and <5  $\mu\text{m}$  fractions.

**Dilution Method.** Phytoplankton growth and mortality were assessed through the use of the modified dilution method (Landry et al 1995). A five-point dilution series was set up with whole seawater (unfiltered) and 0.2 $\mu\text{m}$  diluent to assess phytoplankton growth and mortality. Microzooplankton grazing was assessed with a <200 $\mu\text{m}$  treatment. Incubations were carried out in on deck incubators at environmental light and temperature conditions. Fast rapid rate fluorometry, processed by the Arrigo group, was used to look at the physiological state of the phytoplankton before and after the incubation period. Chl *a* was used as a proxy of cell growth.

**Fluorescently-Labeled Bacteria (FLB) Incubations.** Bacterivory was measured through FLB incubations, where FLB's were added to whole seawater at ~10% of the natural community abundance and incubated for 24-72 hours. 0.2  $\mu\text{m}$  filtered seawater treatments served as a control. The removal rate of these tracer particles will be determined via flow cytometry.

### Preliminary Findings

While the microscopy and flow cytometry will not happen until back at my lab at USC, the chl *a* filters from the dilution experiments were processed while on board with a Turner 10 AU Fluorometer, providing growth and mortality results for the phytoplankton community as a whole.

At the 10 stations, mortality rates ranged from 0.09-0.40  $\text{day}^{-1}$ , with an average of 0.21  $\text{day}^{-1}$ . Unenriched growth rates ranged from -0.06-0.72  $\text{day}^{-1}$ , with an average of 0.42  $\text{day}^{-1}$ . The percent of primary production consumed per day ranged from 17%-105%  $\text{day}^{-1}$ ; interestingly the open water average was 80.8%, while the under-ice average was 49.4%. This difference can be explained by the low growth rates and nitrate drawdown at these open water stations, indicating the phytoplankton community was on a decline during our sampling in these regions.

Grazing in the microzooplankton treatment was less than grazing in the WSW treatment for six of the seven earlier experiments (Stations 008-132, Stn 064 had slightly more grazing in the microzooplankton treatment than the WSW), however, microzooplankton grazing exceeded

grazing in the WSW treatment in the last three experiments (Station 151-209), indicating a shift in community composition. Ciliates/tintinnids were present in all handnet surveys, but dinoflagellates were not present until these later stations. Microscopy counts will further assess this shift in community composition.

Size fractionated chlorophyll analysis of my T0 experiment water revealed that large phytoplankton (>20  $\mu\text{m}$ , namely diatoms), dominated the phytoplankton community at 9 of 10 surveyed stations, with Station 064 being the outlier. The dominance of smaller phytoplankton at Station 064 may explain the aforementioned anomaly (grazing in the microzooplankton treatment exceeding grazing in the whole seawater treatment), as ciliates/tintinnids can feed on these smaller phytoplankton.

# **Lightframe Onsight Keyspecies Investigation (LOKI) of zooplankton**

**Moritz Schmid and Louis Fortier**

*Takuvik Joint International Laboratory (CNRS-University Laval)*

## **Objectives**

The zooplankton imaging component of the SUBICE cruise was based on the LOKI system which can image zooplankton and other particles in the meso and macro range from 180  $\mu\text{m}$  to about 2 cm and at a vertical resolution of about 40 cm. In addition the biological sample was also collected and preserved. The objective of the LOKI-zooplankton component was to (1) sample the overall mesozooplankton assemblage over the entire water column at high vertical resolution in order to determine the coupling of mesozooplankton activity with phytoplankton activity during pre-bloom and under-ice bloom conditions, (2) investigate changes in the vertical distribution of zooplankton over a 72 hour cycle to identify responses to advancing melt pond formation and potential under-ice blooms of phytoplankton and (3) to identify potential thin zooplankton layers through repetitive measurements. The sampling carried out throughout the SUBICE mission varied therefore between full water column stations and ice stations as described in the following paragraphs and is presented in more detail in a table that visualizes the LOKI deployments at each station. Altogether, 64 stations were sampled and 77 single deployments of LOKI made during SUBICE from May 16th, 2014 to June 20th, 2014. Some of the preliminary results, foremost images representing encountered zooplankton species and groups, are presented in this short report. We express our gratitude to the officers and crew of the USCGC *Healy*, who made this cruise a great success.

## **Methods**

At every LOKI deployment, the zooplankton assemblage of the entire water column was imaged using the LOKI system. LOKI provided images of zooplankton and particles linked with environmental data such as chl *a*, temp and salinity from built in sensors and with a vertical resolution of  $\sim 40$  cm. In addition, the biological sample of the whole water column was collected using a bottom net and cod end. LOKI was deployed vertically and towed from  $\sim 5$  m off the bottom, to the ocean surface, at a retrieval rate of  $24 \text{ m min}^{-1}$  (Figure 1). The LOKI net at the top had a mouth opening of 0.75 cm diameter with a 200- $\mu\text{m}$  mesh size net for the collection of the bulk of the meso-, and macrozooplankton size spectrum. After each deployment the biological sample was preserved in seawater and 37% formaldehyde, buffered with borate.



Figure 1. The vertically towed zooplankton imaging system LOKI. Left hand: Schematic drawing of LOKI on the factory built frame. Right hand: LOKI on a new custom built frame made for the SUBICE cruise. Note the net at the top for zooplankton concentration as well as the bottom end which collects the sample after the particles were imaged.

In general, LOKI was deployed once at each full station for the description of the mesozooplankton assemblage and further analysis of the coupling with primary production. At ice stations, LOKI was deployed twice and with about 1 hour in between hauls to identify potential thin zooplankton layers. At the 72 hour ice station, LOKI was deployed every 6 hours and therefore 12 times in total, to investigate the vertical distribution during advancing ice melt conditions. Altogether, LOKI was deployed 77 times at 64 stations.

### **Preliminary Results**

LOKI was able to successfully capture the vertical distribution of organisms ranging in size from 200  $\mu\text{m}$  to about 2 cm and 1.4 million images of plankton and other particles were collected. Some example images are following. All images (e.g. Figure 2) are unchanged and raw footage as recorded by LOKI except for occasional cropping to cut off dark background.

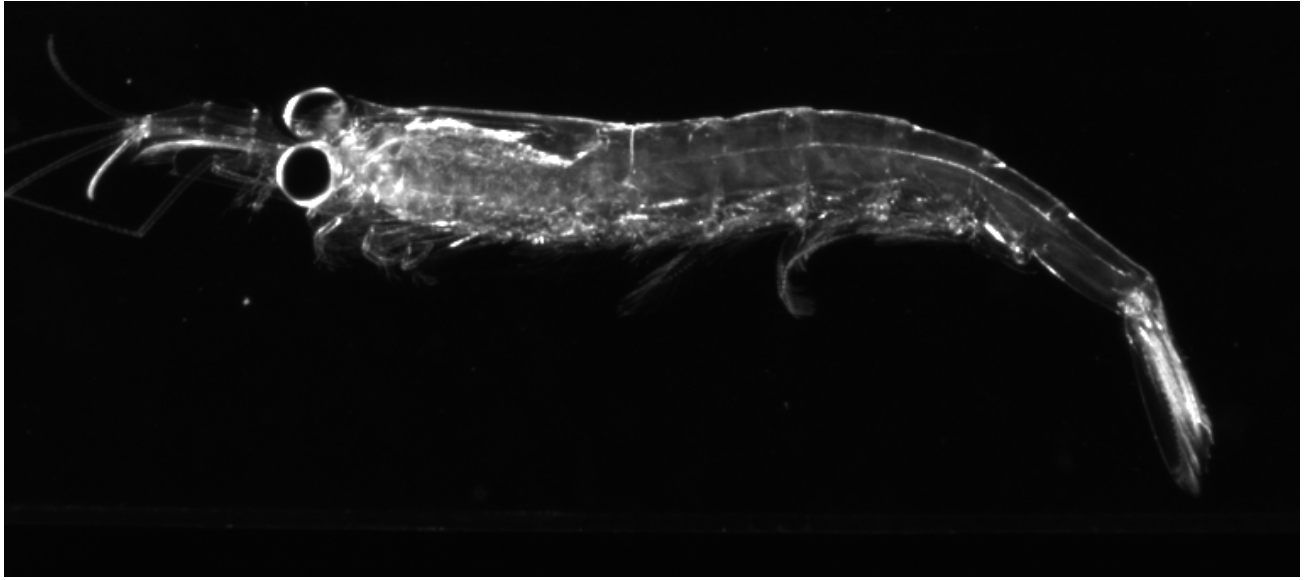


Figure 2. An euphausiid, body length about 1 cm.

Further analysis in the laboratory will include taxonomic analysis of images based on the biological samples that were collected as well as automatic identification to the most detailed taxonomic level possible based on machine learning algorithms. Furthermore, the spatial (horizontal and vertical) as well as temporal coupling of mesozooplankton and phytoplankton distribution will be analyzed and spatially distinct zooplankton populations, based on the taxa encountered throughout the water column, will be identified, as well as potential changes in the vertical distribution of mesozooplankton during the 72 hour ice station.

## Mesozooplankton Abundance and Composition

Carin Ashjian

*Woods Hole Oceanographic Institution*

### Objectives

The primary goal of this component is to describe the abundance and community composition of the mesozooplankton across the Chukchi Sea and the association of those distributions with water masses and circulation. Other objectives include differentiation of the important congeneric copepod species *Calanus glacialis* and *C. marshallae* using molecular techniques and determination if *C. glacialis/marshallae* copepods are utilizing ice algae as a food source in the spring through molecular analysis of their gut contents. Ultimately, the grazing impact on water column chlorophyll and primary production of the mesozooplankton community may be estimated using species abundances, previously determined chlorophyll concentration dependent grazing rates, and observed chlorophyll concentrations and primary production rates.

The distributions of plankton in the Chukchi Sea are closely associated with the dominant current patterns and water mass types. The species composition is strongly influenced by the input of water from the northern Bering Sea through Bering Strait. Injection onto the Chukchi Shelf of plankton originating on the Chukchi/Beaufort Slopes or in the Canada Basin occurs episodically through wind-induced upwelling along the shelf-break and along/in Barrow Canyon. A long-standing question of mine is whether the plankton populations in the Chukchi Sea, particularly of the biomass dominant *C. glacialis/marshallae*, overwinter successfully there or are introduced each spring from the Bering Sea and from the slope/basin to the north. Although zooplankton composition and abundance were documented in May-June 2002 and 2004 as part of the Shelf Basins Interactions Program, sampling for that project was confined to the shelf break, slope, and basin to the north and did not extend over the greater Chukchi Sea such as occurred during the present cruise.

### Methods

Mesozooplankton samples were collected at all ice stations and at “full” stations that were conducted at a subset of the CTD sampling locations. Zooplankton were collected with vertical tows of a paired Bongo net frame equipped with 150 and 500  $\mu\text{m}$  black mesh nets, flow meters, and a time-depth recorder. The nets also were equipped with a flashing strobe that was intended to stun or to impair the vision of krill, decreasing their ability to see the net and to escape and thereby increasing the effectiveness of the nets. Casts were conducted from surface to  $\sim 4$  m off of the seafloor. Samples were examined qualitatively under the microscope and preserved in 4% formalin seawater immediately following collection. Samples will be enumerated in the laboratory for the abundance of the different taxa, species, and life stage if funding to support this analysis can be identified. At ice stations, 1-2 net tows also were conducted using a 1-m<sup>2</sup> ring net equipped with black 250  $\mu\text{m}$  mesh, a time-depth recorder, and a large non-filtering cod end. *C. glacialis/marshallae* from these tows were selected using microscopy and preserved in alcohol for genetic analysis. At a subset of locations, *C. glacialis/marshallae* also were selected using microscopy and frozen for analysis of stable isotopes by T. Schollmeier to determine if the copepods are utilizing ice algae in their diet. The contents of some nets were preserved in EtOH immediately following collection for later molecular analysis to identify their prey composition. At 7 ice stations, egg production experiments were conducted to determine the egg production rate of *C. glacialis/marshallae*. Egg production of these species is believed to largely be dependent on food availability for the copepod. Tows also were conducted at some ice stations

using a 53  $\mu\text{m}$  mesh, 60 cm ring net deployed by hand on a rope to 10 m to collect naupliar stages of *C. glacialis/marshallae*.

### **Preliminary Findings**

Based on qualitative examinations of the samples, *Calanus glacialis/marshallae* were ubiquitous in the Chukchi Sea, with abundances varying with location and with water type. Lowest abundances were seen in the Central Chukchi Sea, with higher abundances to the south and in water likely originating in Herald Valley that was sampled to the NW of Hanna Shoal and along the shelf break. The life stages present varied also with time and space, although adult females, usually ovigerous, were the dominant life stage, and eggs and younger naupliar stages were seen at all locations. In the Herald Valley water and Slope Water to the N of Hanna Shoal, younger copepodid stages (C1-C3) were seen when those stations were occupied in late May, while none were seen in the Central Chukchi during the first portion of the cruise. However, when the stations in the southern portion of the study area were resampled in June, copepodid stages C1-C3 also were observed. The presence of *C. glacialis/marshallae* C1-C3 in the Central Chukchi coincided also with the appearance of high abundances of barnacle nauplii. From these qualitative assessments, it appears that different populations of *C. glacialis/marshallae* were present in the Central Chukchi and in Herald Valley/Canada Basin water in May. By the time the south Central Chukchi Sea stations were re-occupied, water originating to the south and flowing through Bering Strait had spread north to the study area, carrying a Northern Bering Sea population of *C. glacialis/marshallae*, and barnacle nauplii, that had initiated reproduction earlier than the Central Chukchi population. The nearest rocky shores from where the barnacle nauplii could have originated lie in Bering Strait, thus the barnacles serve as a tracer of water entering the Chukchi Sea. Measurements of *C. glacialis/marshallae* egg production rates showed that reproduction was ongoing at rates lower than observed during the SBI program in 2002 and 2004. Egg production rate increased slightly during the period of the cruise and was not correlated with water column chlorophyll. The presence of *C. glacialis/marshallae* eggs and nauplii in the net samples, the ongoing egg production and ovigerous state of the females, and the lack of dependence of EPR on water column chlorophyll suggest that the observed egg production may have been fueled by feeding on ice algae.

Chaetognaths and the copepod *Pseudocalanus* spp. also were ubiquitous in the samples. Other taxa that were observed included polychaete trochophores, chaetognaths, ctenophores, medusa, and pteropods. The Arctic copepod species *C. hyperboreus* was observed only on the northern flank of Hanna Shoal. Euphausiids were observed only in water originating in Herald Valley or at stations located near the Russian Border, suggesting a source in the western side of the Bering Strait. At locations where water recently advected from the Bering Sea was present, the Bering Sea species *Neocalanus* spp. and occasionally *Eucalanus* spp. also were seen.

## Particulate absorption

Atsushi Matsuoka and Marcel Babin

*Takuvik Joint International Laboratory (CNRS-University Laval)*

### Objective

The main objective is to examine optical properties both in open waters and beneath the ice for phytoplankton photosynthetic processes.

### Overview

The light absorbance of particulate matters including phytoplankton ( $\phi$ ) and non-algal particles (NAP) was measured onboard using a spectrophotometer (Varian) equipped with an integrating sphere. Data were scanned from 200 to 800 nm at 1 nm increments based on the quantitative filter technique (QFT: Mitchell and Kiefer, 1988; Mitchell, 1990). Transmission-Reflection method (T-R method: Tassan and Ferrari, 1995, 2002) was adapted for measurements. Sampling was conducted following the NASA Ocean Optics Protocols (Mitchell et al., 2003).

### Methods

Water samples were collected into carboys. These samples were filtered using GF/F filters until when the filters had colors showing optical density (OD) ranging from 0.02 to 0.7 (Tassan and Ferrari, 2002). Absorbance of particles ( $OD_p(\lambda)$ , dimensionless) retained on GF/F filters were then determined from 200 to 800 nm with 1 nm increments using a Varian spectrophotometer with a reference filter pre-soaked in filtered seawater. Absorbance of each sample was recorded in both transmission (T) and reflection (R) modes (T-R method). After  $OD_p(\lambda)$  measurements, phytoplankton pigments retained on the filters were extracted using methanol (Kishino et al., 1985). Absorbance of non-algal particles, NAP ( $OD_{NAP}(\lambda)$ , dimensionless) were determined on the bleached filter. All absorbance data were converted into absorption coefficients of phytoplankton ( $a_\phi(\lambda)$ ,  $m^{-1}$ ) and NAP ( $a_{NAP}(\lambda)$ ,  $m^{-1}$ ) by taking into account pathlength amplification effect caused by highly scattering GF/F filter, known as the  $\beta$ -factor [Mitchell and Kiefer, 1988]. Absorption measurements on 12 UV experiments were also made (Table 2). See cruise report by Arrigo's group for details.

Samples for mycosporine-like amino acids (MAAs), known as sun-screening component produced by phytoplankton, were taken to be analyzed in the laboratory. These concentrations will be quantified using high performance liquid chromatograph (HPLC) after extraction (Matsuoka et al., to be submitted).

Brief summary of sample types and numbers is shown in Tables 1 and 2.

Table 1. Summary of data collected during SubICE

Parameter	Type of sample	Number of sample	Subtotal
ap/MAAs	Water	491/66	557
ap/MAAs	Beneath the ice	18/3	21
ap/MAAs	Bottom ice	27/57	84
ap	Water in melt pond	5/0	5
Total	-	-	667

Table 2. Summary of UV Experiment conducted by Arrigo's group

Platform	Type of experiment	Treatment*	N
Incubation pool	UV experiment on MAAs production	High light and high UV (HH), high light and low UV (HL), low light and low UV (LL), high light and no UV (HN), low light and no UV (LN)	5*12
Total	-	-	60

**Preliminary Findings**

Results will be analyzed after samples are returned to home institution for analysis.

## CDOM absorption

**Sophie Renaut**

*Takuvik Joint International Laboratory (CNRS-University Laval)*

### Objectives

The light absorption properties of particulate and dissolved components (i.e., phytoplankton, NAP, and CDOM) strongly influence the propagation of visible light in oceanic waters, and therefore the accuracy of ocean color algorithms. The variability of light transmission through the ice and the water column could also strongly affect phytoplankton growth. The main objective of this component is to characterize how the presence of CDOM can affect light transmission through the ice and the water column in the early spring ice melt phase.

### Methods

The CDOM absorbance was measured using a liquid core waveguide system, UltraPath (WPIInc) from 200 to 727 nm at 1 nm increments, and using a 2 m optical pathlength for all the samples.

The samples were collected from the CTD bottles at 4-11 depths and from the ice station (bottom of the ice cores, water beneath the ice, and melt pond). They were collected into MilliQ pre-rinsed 250 ml amber glass bottles. Samples were filtered immediately (or as soon as possible for the ice station) after collection, in dim light, using 0.2 mm Millipore filters pre-rinsed with 200 ml of Milli-Q water. Filtered samples were then pumped into the sample optical cell of the Ultrapath instrument. Absorbance spectra were measured with reference to a salt solution (the salinity of the reference was adjusted to that of the sample as far as possible,  $\pm 2$ ). This salt solution was prepared with Milli-Q water and pre-burned NaCl (i.e., NaCl was pre-burned by placing it in an oven at 400°C for at least 4 hours). Between each measurement, the sample cell was cleaned several times, successively with detergent (citranox), methanol 50%, HCl 0.1 N, and Milli-Q water.

The presence of micro bubbles in the sample cell was also minimized using a peristaltic pump. They could induce significant absorption, detectable in the infrared, and therefore the corresponding absorption spectra would be discarded.

Water was also sampled and stored at certain stations for further CDOM fluorescence analysis.

Table 1. Summary of data collected during SUBICE 2014.

	CDOM absorption		CDOM fluorescence	
Platform	Nbr. stations	Nbr. samples	Nbr. stations	Nbr. samples
CTD-bottles	120	606	27	40
ice core	19	19	2	2
beneath the ice	17	17	3	5
melt pond	2	2	0	0
Total	-	644	-	47

### Preliminary findings

Due to a lack of time onboard, a subsequent data analysis has to be performed after the cruise.

## **Marine Optics (AOP and IOP profiles) and UVP imagery and particles size distribution profiles**

**Guislain Bécu, Joannie Ferland, Atsushi Matsuoka**  
*Takuvik Joint International Laboratory (CNRS-University Laval)*

### **Objectives**

This report describes two data types that were acquired during the SUBICE 2014 cruise, namely the marine optics data and particles and zooplankton imagery data.

### **AOP / IOP measurements**

The first set of data, i.e. the marine optics, includes apparent optical properties data (the so-called AOP data), as well as inherent optical properties (the so-called IOP data). The AOP are the optical properties of the seawater that depend on the environmental conditions, like the nebulosity, the sun elevation, or especially in the Chukchi Sea, the presence of sea-ice and snow between the seawater and the atmosphere. For example, the spectral downwelling irradiance, or  $E_d(z)$ , is an apparent optical property. The IOP are the optical properties of the seawater that do not depend on the environmental conditions. For example, the seawater absorption, or  $a(z)$ , is an inherent optical property.

Usually, AOP and IOP measurements are performed *in situ* mainly to calibrate vicariously and / or validate satellite observations of the Ocean Color. Of course, with the presence of sea-ice, the satellite observations are not useful, but here the AOP and IOP measurements were acquired to complement the sea-ice optical properties data set, acquired by Don Perovich's team. Indeed, the light field that arrives at the bottom of the atmosphere is changed when crossing the snow / sea-ice interface, but is also further modified in the water column. Describing it from right underneath the ice cover (i.e. from the top of the water column) down to the seabed (or down to the depth at which no light is barely available any more for deeper stations) is crucial to characterize the amount and the spectral quality of the light available for the phytoplankton to grow during a spring bloom. While the AOP data describes perfectly this light field, the IOP complement these data with parameters like absorption and attenuation spectra or particle size distributions to characterize the seawater constituents.

### **UVP imagery measurements**

The second set of data, i.e. the particles and zooplankton imagery data, was deployed along with the rosette carousel to describe the particle size distribution profiles, including large zooplankton ones, to help characterizing the vertical fluxes (especially of carbon).

### **Methods**

#### **AOP / IOP measurements**

Apparent and inherent optical properties, i.e. AOPs and IOPs, were measured *in situ* from a 10 inches hole drilled in the ice at every single ice station during the SUBICE 2014 cruise.

Inherent optical properties profiles were measured using a so-called "IOP frame" (see photographs on figure 1, including the following physical and optical sensors: a Seabrid Electronics FastCat 49 CTD, an WETLabs Inc. "AC-S" hyperspectral absorption and attenuation meter (in the visible part of the spectrum), a Sequoia Scientific Inc. "LISST" particle size distribution sensor (32 sizes bins ranging from 1.25  $\mu\text{m}$  to 250  $\mu\text{m}$ ), a first WETLabs Inc. ECO puck sensor fitted with a Chl-a fluorescence probe, a CDOM fluorescence probe and a 700 nm

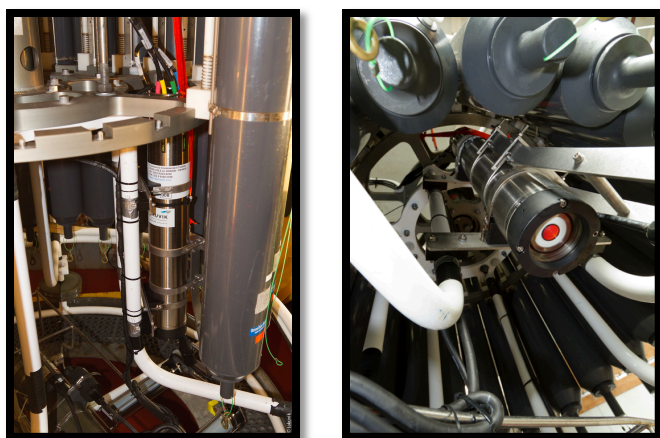
backscattering probe, and a second WETLabs Inc. ECO puck sensor fitted with 3 backscattering probes at 720, 770 and 870 nm.

The IOP frame was lowered in the hole with the help of a tripod and a battery-powered pulley, from underneath the hole down to the seabed. The maximum cable length of 220 m allowed sampling all the stations down to the seabed. As opposite to the AOP data sensor, the IOP frame can be lowered below the depth at which no natural light is barely available, as all of its optical sensors are active optical sensors, i.e. they use a light source to perform their measurements. The AOP sensors are passive optical ones, i.e. they measure the ambient light.

Apparent optical properties were measured using the so-called “IcePro” version of the C-OPS (“Compact-Optical Profiling System) from Biospherical Instruments Inc. The IcePro consists of a two half-cylindrical foam collars system designed to deploy the optical heads of the C-OPS through a 10 in hole drilled in the ice floe (The C-OPS system looks otherwise like a kite and would require more holes to be drilled to be deployed). For the SUBICE 2014 cruise, two irradiance sensors were mounted on the IcePro frame. They are measuring the spectral upwelling ( $E_u(z)$ ) and the spectral downwelling ( $E_d(z)$ ) irradiance profiles at the same 19 wavelengths (namely 380, 395, 412, 443, 465, 490, 510, 532, 555, 560, 589, 625, 665, 683, 694, 710, 765, 780 and 875 nm), from just underneath the ice hole down to either the seabed or down to the water depth at which no signal was recorded any more (whichever comes first). An atmospheric reference sensor measured the downwelling irradiance at the bottom of the atmosphere. Next to the atmospheric unit, a GPS receiver allows the geo-localization of the measurements, and a stepper motor driving a shade band above the atmospheric unit allows for further atmospheric analysis (in particular it allows the characterization of direct vs. diffuse sky irradiances). Also, when time allowed, the AOP wet unit was left at a constant depth (usually approximately 5 meters below the ice) for a continuous low frequency (0.1 Hz instead of 15 Hz for the profiling mode) acquisition of upwelling irradiance, downwelling irradiance and bottom of the atmosphere irradiance.

### Particles and Zooplankton imagery

Particles and zooplankton imagery was also performed using an underwater vision profiler (UVP) instrument, fitted on the rosette frame. The UVP5 is an instrument designed to take pictures of a slice of water lighted by 2 rows of flashing LEDs while profiling or while being



moored (profiling with the rosette during the SUBICE 2014 cruise). An image processing performed either onboard while profiling, or in delayed mode after data recovery (at the user's convenience), estimates the particles size distribution and stores vignettes of the particles found in the images. The pixel size of the camera is approximately 150  $\mu\text{m}$ , so that the particles detected by the UVP are ranging from 150 microns up to few centimeters. The photographs on the figure 1 shows the UVP mounted on a rosette carousel (on another cruise than the SUBICE one).

Figure 1. The UVP imagery system fitted on a rosette carousel.

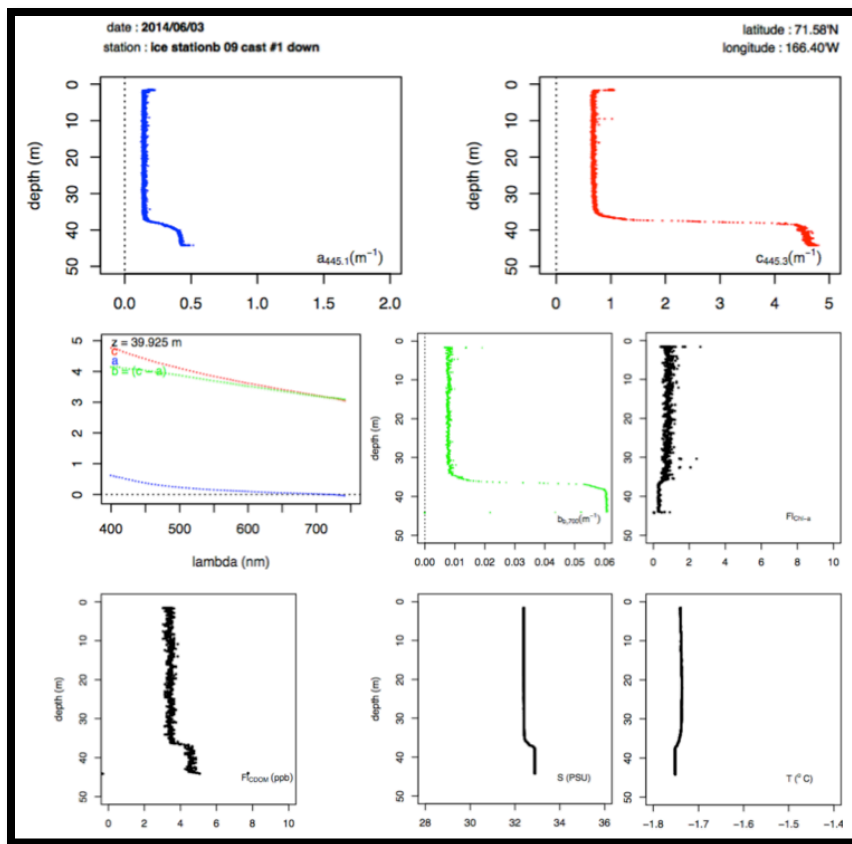
Among the 230 stations (approximately 250 casts), 230 UVP profiles have been acquired, along

with 91 AOP profiles, 20 AOP continuous low-frequency measurements at a constant depth, 26 additional AOP sky measurements, and 62 IOP profiles.

### Preliminary Findings

Note that this section gives very preliminary results, obtained after a rough quality control. For the AOP data, for example, several cross calibrations and dark current time series have been performed but not analyzed yet – for the IOP data, blank signal (with pure water) data have been acquired every other day (when no ice station was happening mainly), but were not analyzed yet, as well. All these quality controls have to be carried on after the cruise and may impact the results shown here.

AOP / IOP acquisition. For illustrative purposes, the figure 2 below shows a typical IOP cast, including a profile of absorption ( $a$ ) and attenuation ( $c$ ) at 445 nm, a spectrum of  $a$  and  $c$  (and thus the light scattering  $b = c - a$ ) at approximately 40 m deep, a profile of particulate



backscattering coefficient at 700 nm, a profile of chl- $a$  fluorescence, a profile of CDOM fluorescence, a profile of temperature as well as a profile of temperature, all taken at the ice station #9 (CTD station number 104). These profiles are rather typical for the 7 last ice stations that were sampled (roughly half of them), i.e. starting with a homogeneous water column from under the ice down to between 5 and 15 m above the seabed, where a bottom layer (nepheloid layer?) is clearly visible. Indeed, the light absorption and especially the light attenuation are constant and low from the surface down to

Figure 2. A typical IOP cast.

approximately 38 m, where they increase dramatically within one or two meters, and stay very high down to the seabed. In this bottom layer, the fluorescence of the chlorophyll- $a$  is decreasing (even if not very large above) and the fluorescence of the CDOM is increasing, slightly as well. The physical sensors ( $T$  and  $S$ ) show that the bottom layer is a different water mass, as it is saltier and colder.

Figure 3 below show a typical AOP profile of downwelling irradiance for all the 19 wavelengths. The data shown of this figure is also from the ice station #9 (CTD station #104). Again, a 5 to 10 meters layer located at the bottom of the water column (i.e. just above the

seabed) is attenuating the light more drastically than the homogeneous layer that is just above it (note the logarithmic x-axis). This is consistent with the IOP profiles.

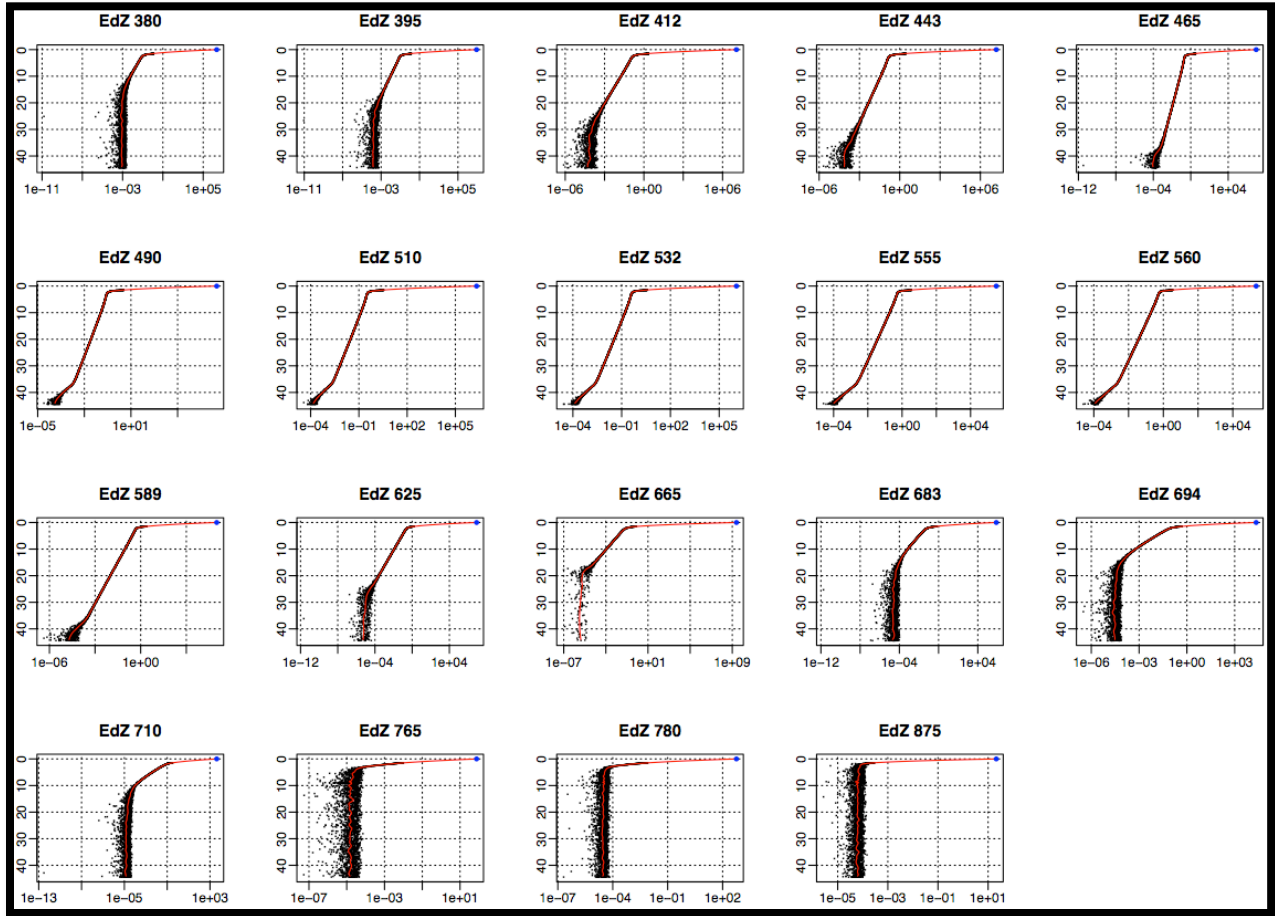


Figure 3. Profiles of downwelling irradiance from a Typical AOP cast.

Due to a lack of time onboard, no further data processing could be completed during the cruise, and a subsequent data analysis has to be performed after the cruise, when back at the University Laval. No conclusion can therefore be drawn.

## **Van Veen grabs and IP<sub>25</sub> sampling**

**Tanja Schollmeier**

*University of Alaska, Fairbanks*

### **Objectives**

The objectives of this research were to sample the ice cores, water, surface sediment and in- and epifauna for IP<sub>25</sub>. IP<sub>25</sub> (Ice Proxy with a 25 carbon chain) is a biomarker, which is produced by ice algae. This biomarker is only produced in conditions where the algae are growing under the ice and not in open water conditions. The ongoing reduction of seasonal sea ice coverage in the Chukchi Sea due to global climatic changes is projected to dramatically reduce the contribution of primary production from sea ice algae to the marine ecosystem. The shift to a system dominated by pelagically-derived production may affect benthic organisms on the Chukchi shelf that are dependent on the early-season food pulse currently provided by sea ice algae. This project will track IP<sub>25</sub> from its origin in ice algae, into the water column, into the sediment and into benthic feeding organisms. Results of this project will reveal how ice algae are utilized in the benthos and will enhance our understanding of how climate change may affect the benthos and subsequently other ecosystems.

### **Methods**

Benthic organisms were collected with Van Veen grabs at every station they were found. Collected individuals were identified and frozen whole for later analysis. Additionally, surface sediment samples and phytoplankton samples were collected from the Van Veen and from Niskin bottles attached to a CTD (Conductivity, Temperature, Depth recorder) rosette, respectively. These samples were also frozen like the benthic organisms. At ice stations ice cores of the bottom 10 cm were collected for ice algae analysis and like the phytoplankton were filtered onto GF/F filters. Additionally pore water samples of partial drilled ice cores were collected at various depths for later stable isotopic analysis of the dissolved inorganic carbon. The pore water samples were collected in crimp top vials, stabilized with saturated mercuric chloride solution and parafilm for later analysis.

All samples were frozen for later analysis. In the lab analysis following samples will be freeze dried and homogenized. For the extraction process a 2:1 dichloromethane (DCM) and methanol (MeOH) will be used as a solvent system in addition to two internal standards used that will allow later IP<sub>25</sub> quantification. After this initial extraction the total organic extract (TOE) is weighed after nitrogen evaporation before purification. The TOE is separated by column chromatography, which eludes non-polar hydrocarbons including IP<sub>25</sub>. Following column chromatography, eluded compounds will be analyzed using gas chromatography-mass spectrometry (GC-MS) analysis at the Kodiak Seafood and Marine Science Center (UAF).

### **Preliminary Findings**

Results will be analyzed after samples are returned to home institution for analysis.

## Outreach activities during SUBICE 2014

**Ben Harden (Coordinator, documentarian), Dallas Murphy (Writer), Amanda Kowalski (Photographer, videographer), Chelsea Clarke (Artist), Jan Nash-Arrigo (Teacher), Jody Sperlina (choreographer)**

### Objective

Our primary goal as an outreach team was to communicate the science and life aboard the icebreaker *Healy* during the SUBICE expedition through a range of mediums by posting to the website [www.arcticspring.org](http://www.arcticspring.org). The secondary goal was to gather materials and ideas for a body of work upon our return to shore.

### Activities

We documented the activities on cruise in a range of mediums: prose, photos, video, audio, art, dance and through student interactions. Dallas wrote dispatches every other day. Amanda illustrated these with her photos and produced other photo galleries. Ben and Amanda documented the expedition through various multimedia products. Jan wrote posts for the website, conducted interviews with scientists, and answered questions sent in by elementary school children. Chelsea researched plankton and Arctic life and produced drawings and sketches that both demonstrated the life in the north and gave people insight into the artistic method. Jody danced at 12 ice stations and documented this for future dissemination.

The primary objective can be divided into two components: production of the content and reception of the content. In terms of production, we posted 90 articles to the website across all the mediums. This was a success in and of itself. Furthermore, the site was well received. We had an average of 1000 hits per day throughout the expedition (Figure 1). There was some temporal variability in this, with the most hits coming in week three of the expedition (peaking at over 1600 hits per day). We need to undertake further analysis to understand this, but a likely reason is that the school year was ending in many places at that time, hence we lost a sizeable part of our audience.

Over the course of the expedition we received nearly 100 online comments on the articles, and attempted to respond to each one. In addition, we advertised the site through social media, at times being re-tweeted to 80,000 people and getting thousands of “likes” on Facebook through the coastguard and institutional social media. Again, we need to ascertain which promotional activities were the most successful in engaging a following of SUBICE.

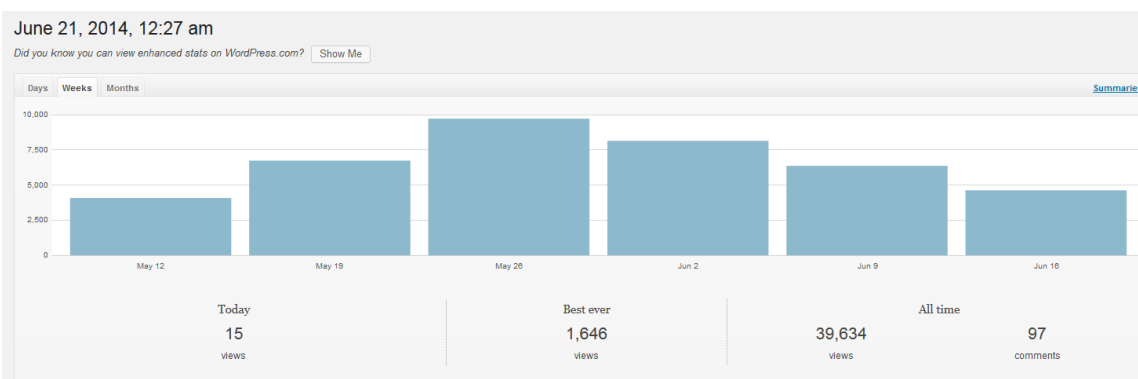


Figure 1. Number of page loads per week for the 6 weeks of the SUBICE expedition.

## **Conclusions**

The outreach activities spanned a broad range of mediums and the website was populated with a large variety of content that reached a great many people. Emphasis was placed both on the science being done as well as on Coast Guard activities and life aboard *Healy*. The outreach team will now go forward with individual projects such as dance performances, art shows, radio pitching, and magazine articles to extend the reach of this expedition beyond the timeframe of the cruise.